Contents lists available at ScienceDirect

Atmospheric Environment

Observing decoupling processes of NO$_2$ pollution and GDP growth based on satellite observations for Los Angeles and Tokyo

Renée Bichler [a,b,*], Stefan Samuel Schönebeck [a,c], Michael Bittner [a,b]

[a] German Remote Sensing Data Center, German Aerospace Center, Oberpfaffenhofen, Germany
[b] Institute of Physics, University of Augsburg, Augsburg, Germany
[c] Institute of Geography, University of Würzburg, Würzburg, Germany Now at Faculty of Plastics Engineering and Surveying, Technical University of Applied Sciences Würzburg-Schweinfurt, Germany

HIGHLIGHTS

● Long-term time series analysis for Los Angeles and Tokyo using spectral analysis methods.
● Decoupling process between NO$_2$ pollution and GDP for Los Angeles and Tokyo.
● Comparison between NO$_2$ variability and air pollution control measures.

ABSTRACT

Nitrogen dioxide (NO$_2$) pollution is mainly caused by anthropogenic processes such as burning of fossil fuels. Due to its severe impact on health as well as the environment in general, it is important to monitor the amount of NO$_2$ pollution especially in areas with a high population density. Therefore, the aim of this study is to investigate to what extent spatiotemporal fluctuations in the tropospheric NO$_2$ column density can map variations in economic output. To do so, we analyzed satellite based tropospheric NO$_2$ column observations obtained from the ERS-2, ENVISAT, MetOp-A and MetOp-B satellite missions covering the period from 1996 to 2017 for Tokyo, Japan and Los Angeles, United States. Within our studies, a harmonic analysis was carried out in order to exclude meteorological influences. Afterwards, the NO$_2$ time series were further investigated through a wavelet analysis method to characterize the fluctuations, that is the temporal variability of the NO$_2$. These fluctuations have been shown to be a particularly sensitive measure of the change in NO$_2$ pollution. We further use the gross domestic product (GDP) for the metropolitan areas as an indicator for economic performance. The results for the study area of Los Angeles shows a substantial reduction in NO$_2$ variability starting in 2007. The NO$_2$ variability for the period during the global financial crisis (December 2007–April 2012), dropped by around 77% in comparison to the previous period (January 1997–November 2007). However, a second period from May 2012 to December 2016 presents a further reduction of the NO$_2$ variability of around 82% in contrast to the period from 2007 to 2012. Contrary to this, continuous economic growth can be observed during the second period. A similar picture emerges for the metropolitan region of Tokyo. A significant decline in NO$_2$ variability of around 73% can be detected from October 2003 to January 2012. Additionally, a second period with a strong decline in NO$_2$ variability of around 80% can be identified from February 2012 to December 2016. A plunge in GDP during 2008 reflects that year's global financial crisis, but cannot independently explain the following sharp decline in NO$_2$ variability. Those results suggest that Tokyo as well as Los Angeles managed to substantially decouple its NO$_2$ pollution from the economic growth due to strict air quality policies.

1. Introduction

Nitrogen oxides (the sum of nitrogen monoxide (NO) and dioxide NO$_2$, often referred to as NO$_x$) are mainly produced by anthropogenic processes such as fossil fuel combustion as the most dominant source, lightning and by soil release and biomass burning (see for example

---

Seinfeld and Pandis, 2016 or Brasseur and Jacob, 2017 for a comprehensive description). As a result of nitrogen dioxide's (NO_2) high reactivity as a trace gas (depending on the dominant meteorological characteristics, other trace gases, as well as the height in the atmosphere), the lifetime of NO_2 can vary between some hours in the lower troposphere or even up to days near the tropopause (Pérez-Invernón et al., 2022; Liu et al., 2016; Shah et al., 2020; Levy II et al., 1999).

Even though NO_2 can be transported over certain distances by winds depending on its given lifetime, it is possible to draw - to some extent - conclusions about the sources of NO_2 emissions. Many studies have been conducted on this in recent years. For example, Müller et al. (2022) mapped areas of systematically higher and lower tropospheric NO_2 pollution over Germany based on annual mean Sentinel-5 Precursor (Sentinel-5P) with TROPOspheric Monitoring Instrument (TROPOMI) data. They find that higher NO_2 pollution appear over highly populated urban areas and over rural areas close to power stations at opencast lignite mines whereas lower pollution occurs over rural areas. Similarly, Beirle et al. (2019) demonstrated that by using Sentinel-5P NO_2 and wind data it is possible to create top-down emission maps without using chemical transport models. The authors used their approach to analyze point sources which emit NO_x emissions such as power plants or cement plants in Riyadh, Germany and South Africa. Such results underline the impact of anthropogenic activity on air pollution. This means that observing the spatiotemporal distribution of NO_2 pollution allows conclusions to be drawn about the economic activity in a region. Due to their global coverage, satellite-based observations would therefore enable such studies in almost any place on Earth. Various studies support this approach. Hilboll et al. (2013) for example used the European Remote-sensing Satellite-2 (ERS-2) with the Global Ozone Monitoring Experiment (GOME), the Environmental Satellite (ENVISAT) with the Scanning Imaging Absorption Spectrometer for Atmospheric Cartography (SCIAMACHY), the Earth Observation System – Aura (Aura) with the Ozone Monitoring Instrument (OMI), and the Meteorological Operational Satellite-A (MetOp-A) with the Global Ozone Monitoring Experiment-2 (GOME-2) data from 1996 to 2011 to analyze the NO_2 long-term trends for various megacities around the world. The authors also conclude that there has been a decrease in NO_2 pollution over industrialized countries such as the USA, Europe, Japan, or Australia for instance. In contrast, megacities in China, India or the Middle East presented increasing trends. Castellanos and Boersma (2012), Russell et al. (2012), Vrekoussis et al. (2013), Lelieveld et al. (2015), Tong et al. (2015), as well as Cui et al. (2022) addressed the relationship between economic activity and air pollution. They not only concluded that policy measures were responsible to significant reductions in NO_2 pollution but also that severe economic events such as the global financial crisis in 2008, the recent COVID-19 pandemic in 2019–2022, as well as humanitarian catastrophes such as armed conflicts had an impact on air quality.

Moreover, decreases in human activity caused by lockdowns during the COVID-19 pandemic that began in 2019 has a significant impact on air quality (see for example Liu et al. (2020), Goldberg et al. (2020), Zhang et al. (2020), Liu et al. (2021), Voigt et al. (2022), Le Quéré et al. (2020), Filonchyk and Peterson (2020), and Filonchyk et al. (2021) as well as references therein).

In Bichler and Bittner (2022), we analyzed the development of the Italian GDP, as reported by the Organization for Economic Co-operation and Development (OECD), against NO_2 pollution based on satellite observations from ERS-2/GOME, ENVISAT/SCIAMACHY, MetOp-A/GOME-2, and MetOp-B/GOME-2 in the Po Valley in northern Italy. We used the intensity of temporal fluctuations in NO_2 pollution based on wavelet analysis as a very sensitive measure of systematic changes in NO_2 burden. We found that from mid-2007 to mid-2013 a significant reduction in NO_2 variability took place while at the same time Italy faced severe declines in GDP development. Therefore, we concluded that the fluctuations in NO_2 pollution provide a very sensitive measure for tracking fluctuations in economic activity. Correspondingly,

a study by Al Yammahi and Aung (2022) shows similar findings about the impact of the COVID-19 lockdown on the NO_2 variability over the United Arab Emirates based on a wavelet analysis.

Another recent study by Jia et al. (2022) who studied the NO_2 tropospheric vertical column density (VCD) with OMI data as well as the economic development in China concluded that with an increasing industrial electricity consumption of one billion kWh, the tropospheric NO_2 VCD increases by 25% for Nanjing, 12% for Suzhou, and 59% for Xuzhou. Furthermore, the study found that an increase by one billion USD in total exports leads to an increase of 15% and 6% of tropospheric NO_2 VCD for Nanjing and Suzhou. It should be noted that the influence of economic activity on air quality has been investigated in many studies such as Grossman and Krueger (1995), Dinda et al. (2000), Jiang et al. (2020), Hassler et al. (2016), and Tong et al. (2015). It can thus be concluded that air quality and economic activity are coupled in a fossil-based economy.

In this study we focus on the expectation that a decoupling process of the relationship between NO_2 pollution and economic growth occurs when economic development is either made more sustainable (e.g. electromobility, renewable energy) and/or when the use of pollution filters is increased due to political specifications such as air pollution control mechanisms. Regarding a decoupling process between air pollution and economic growth see for example Wu et al. (2022), Li et al. (2021), Shen et al. (2021), Fang and Yu (2021), Yu and Fang (2021) and references therein. What remains unanswered is how well processes of decoupling economic activity and air quality (in our case we focus on NO_2) can be recorded from satellite observations.

Research and monitoring of air pollution exposure are important due its harmful impacts on human health. The World Health Organization (WHO) reports that 4.2 million premature deaths were estimated in 2016 due to ambient air pollution (WHO, 2022). Konduracka and Rostoff (2022) analyzed published literature regarding the relationship between outdoor air pollution and cardiovascular morbidity as well as mortality over a period of 30 years. The authors concluded that exposure to pollutants such as particulate matter (PM) as well as other gaseous pollutants are substantial contributors for cardiovascular morbidity and mortality. Furthermore, the authors emphasize that a vast amount of studies show that the health effects remain serious even below defined limits by the European Union (EU) or the WHO. Nevertheless, air pollution not only affects the health of living beings on Earth, it can also damage sensitive ecosystems (Itoh et al., 2021).

In this study, two prominent regions – Los Angeles, USA and Tokyo, JPN – are examined. The changes in NO_2 pollution are characterized by the NO_2 fluctuations, the NO_2 trend, and the change in characteristics of the NO_2 annual variation in terms of the amplitudes. Therefore, a self-consistent 21-year long time series by Georgoulias et al. (2019) is analyzed. This time series is based on four different satellite instruments such as GOME/ERS-2, SCIAMACHY/ENVISAT, GOME-2/MetOp-A, and GOME-2/MetOp-B. In comparison to other studies, we used advanced spectral analysis methods and satellite observations to investigate worldwide decoupling processes between NO_2 pollution and economic activity which could support the United Nations Sustainable Development Goals (UN SDGs) on a global scale and the European Green Deal at the regional scale.

The paper is organized as follows, Section 2 details sources of data, Section 3 explains the methods, in Section 4 describes the results, Section 5 includes the interpretation and discussion our findings with the literature review, and Section 6 covers our summary and conclusion. Sections 7 and 8 include an acknowledgement as well as our references.

2. Data

2.1. Tropospheric NO_2 vertical column density

Since the data was taken by four different satellites which include ERS-2/GOME, ENVISAT/SCIAMACHY, MetOp-A, and MetOp-B/GOME-

2, the self-consistent data product generated by Georgoulias et al. (2019) is used to avoid influences like different spatial resolution and so forth. Therefore, Georgoulias et al. applied a three-step procedure on the GOME (April 1996 to June 2003), SCIAMACHY (July 2002 to March 2012), GOME-2A (January 2007 to September 2017), and GOME-2B (January 2013 to September 2017) TM4NO2A version 2.3 data products which are available from the Royal Netherlands Meteorological Institute (KNMI). The authors procedure is based on methods of Hilboll et al. (2013) and Geddes et al. (2016). In a first step, Georgoulias et al. applied a spatial resolution correction regarding the different horizontal resolution of GOME and SCIAMACHY. Afterwards a shift correction is applied (step 2) to consider the instrumental biases between the different measurement instruments. In a third step, a seasonal amplitude correction is carried out. Detailed information about the compilation of the 21-year self-consistent data can be found in Georgoulias et al. (2019) and references therein. The gridded vertical tropospheric NO_2 column density data used in our study (Merged TM4NO2A version 2.3) is publicly available on the Tropospheric Emission Monitoring Internet Service (TEMIS) website (www.temis.nl) and covers a period from 1996 to 2017. It should be mentioned that there are no monthly mean values for January 1998. Those values were therefore interpolated linearly.

GOME, SCIAMACHY, and GOME-2 are Nadir-viewing passive measurement instruments that observe the reflected UV–visible sunlight in the morning (equator crossing times between about 09:30 LT and 10:30 LT). By comparing the spectrum gained from the reflected sunlight with the spectrum of the sunlight itself, it is possible to draw conclusions
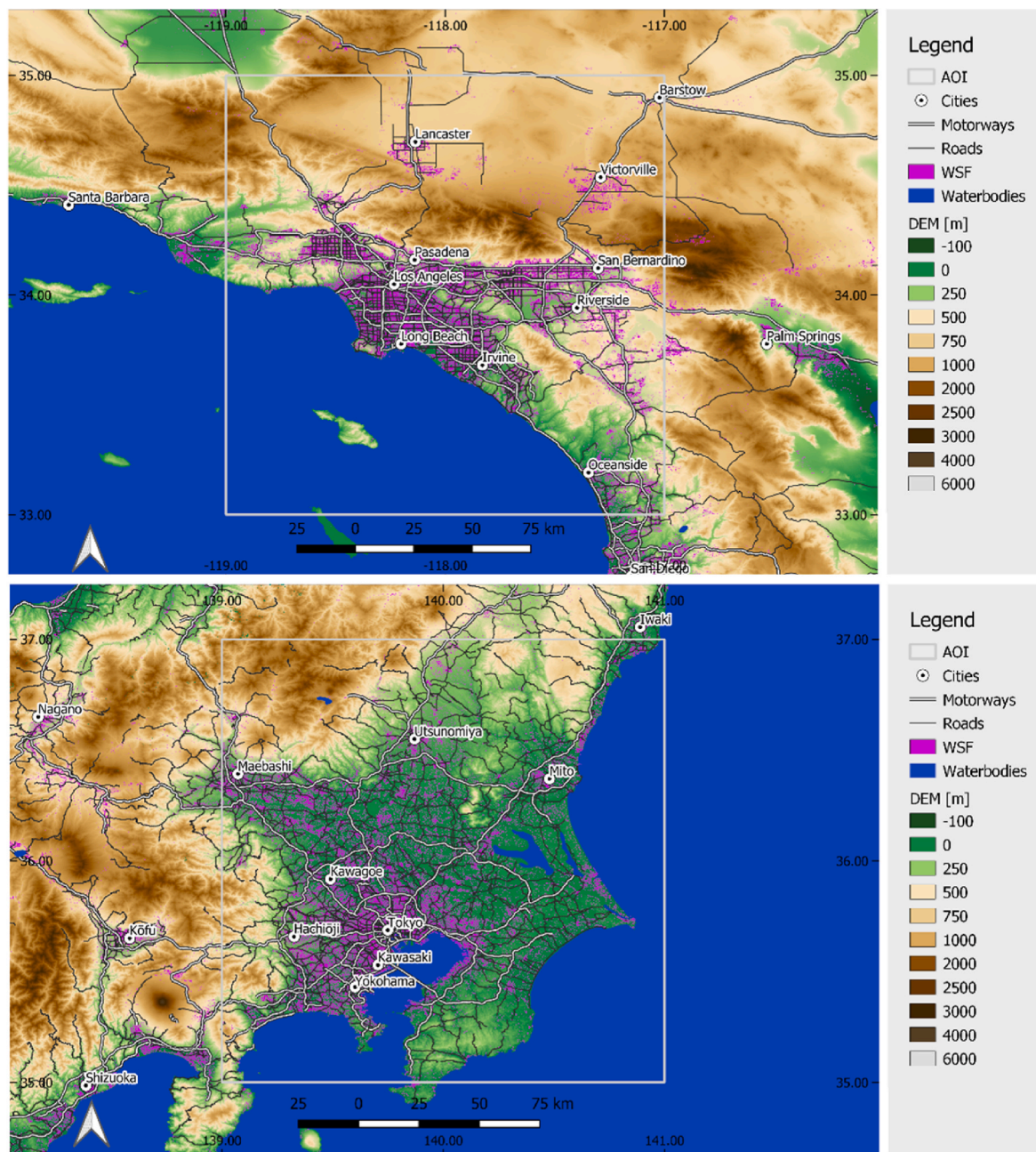

Fig. 1. Topographic Map of the study areas (A) Los Angeles, California, USA (Latitudes: 33°–35°, Longitudes: 117° − −119°) and (B) Tokyo, Japan (Latitudes: 35°–37°, Longitudes: 139° − 141°). The maps also include information about the Digital Elevation Model (DEM) and the World Settlement Footprint (WSF). Sources: World Settlement Footprint, 2019; OpenStreetMap (2023); USGS SRTM 1 Arc-Second Global, 2018; Made with Natural Earth, 2023; GSHHG, 2017; Wessel and Smith, 1996; EPSG: 4326.

about the amount of trace gases in the atmosphere. The VCD is thereby a product from the slant column density (SCD) and the influence of the air-mass factor (AMF). The tropospheric NO_2 VCD can be derived from this. Further information about the measurement instruments can be found in Burrows et al. (1995, 1999), Bovensmann et al. (1999), and Munro et al. (2016) as well as references given therein.

NO$_2$ is well-known to show a pronounced diurnal cycle. We therefore did not consider the observations from TROPOMI/Sentinel-5P and OMI/Aura in our study. These satellites have significantly different equator crossing times (Boersma et al., 2008; Georgoulias et al., 2019).

As aforementioned, the instruments used in our study deliver the tropospheric NO_2 VCD. They do not provide the surface concentration of NO_2. In fact, the majority of the signals measured stem from higher altitudes. See for instance the book of Rodgers (2000), which addresses inverse methods for atmospheric soundings and the work of Eskes and Boersma (2003) who concentrate on averaging kernels for the Differential Optical Absorption Spectroscopy (DOAS) total-column satellite retrievals.

2.2. Areas of interest

A first study area (Fig. 1A) covers the metropolitan area of Los Angeles in Los Angeles County with around 10 million inhabitants as well as Ventura County (~844,000 inhabitants), Orange County (~3,2 million inhabitants), and parts of San Bernardino County (United States Census Bureau, April 1, 2020). The area of interest borders the Pacific Ocean in the south and the San Gabriel Mountains in the north. Due to the location close to the ocean, a sea breeze/land breeze circulation can occur which impacts the air pollution in the city. The land/sea breeze circulation has a diurnal cycle which, in the case of Los Angeles, causes a sea wind in the morning that brings cold Pacific air into the city. At nighttime, the circulation changes into a land breeze and therefore transports air pollution – which are produced during the day in the city – to the Santa Monica Bay. This phenomenon and the impacts on several pollutants has been studied by Wagner et al. (2012) and Jury (2020) as well as references therein. With this information in mind it should be noted that the satellite observations are taken in the mornings and thereby the polluted air might be influenced by fresh air due to the sea breeze. Wagner et al. (2012) and Brioude et al. (2013) also point out that besides land/sea breezes, there are other influencing factors on pollution transport such as the localized "Catalina" eddy wind pattern in this area, as well as the impact of the surrounding terrain and therefore the

upslope transportation of air pollutants. Moreover, Jury (2020) emphasizes that 85% of the precipitation is below 0.2 mm/day and 82% of the analyzed wind speed over Los Angeles is below 2 m/s thus conditions are ideal for the development of thermal inversions. Referring to the www.climate-data.org, the highest temperatures occur in July, August, and September with around 32 °C on average. The highest amount of precipitation with an average of 84 mm and 89 mm can be observed in January and February.

Our second study area (Fig. 1B) covers the Tokyo metropolitan region in Japan at 35°N to 37°N and 139°E to 141°E. According to Tokyo's Statistical Tokyo Statistical Yearbook, 2020, around 14 million inhabitants live in the megacity. In terms of the climatology the maximum temperatures are usually reached from June to September with an average of around 27 °C. The maximum values of precipitation are reached in September and October with around 200 mm (see www.climate-data.org). In regards to the topography, the study area borders the Pacific Ocean in the east and south, and the Akaishi mountains in the west. Due to thermal differences between land and sea during the day, a sea breeze occurs throughout the day and a land wind through the night which can have an impact on air pollution. (Itoh et al., 2021).

Each study area has different meteorological characteristics such as land/sea breeze circulations, the monsoon or frequently occurring temperature inversions for instance. Since, for example, wind and/or precipitation influence the degree of pollution in the air, it is important to briefly understand the meteorological peculiarities in order to comprehend the self-cleaning process of the atmosphere in a certain area. By the self-cleaning process of the atmosphere we mean the influence of meteorology regarding to air pollution that lead to a reduction in NO_2 pollution. There are therefore study areas where the atmosphere influences the reduction of NO_2 pollution more than others. Therefore, for example, the pollution levels for the same NO_2 emitters can be different. Further investigations regarding the meteorological influences during the examined period for each study area can be found in section 2.3 Meteorological Data.

2.3. Gross domestic product

The GDP for the metropolitan areas Los Angeles and Tokyo is taken from the OECD. The GDP data is made available for free and offers information about the annual development of metropolitan areas all over the world (OECD, 2022).

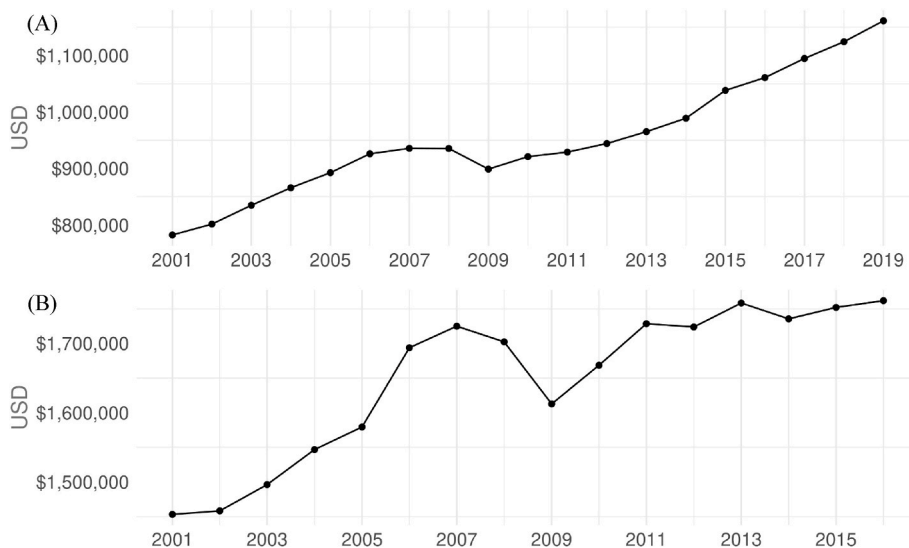Both areas of interest, Los Angeles and Tokyo, show a continuous

Fig. 2. Temporal development of the GDP for the metropolitan areas (A) Los Angeles from 2001 to 2019, and (B) Tokyo from 2001 to 2016. Source: Draft produced from OECD (2022), Data table: CITIES, Metropolitan areas, Economy, GDP (Million USD, constant prices, constant PPP, base year 2015).

growth of the GDP from 2001 to 2007. When the global financial crisis took place in 2008 a drop of about 37.000 USD (2008: 935.289 2009: 898.771) for Los Angeles and around 90.000 USD (2008: 1.702.305, 2009: 1.612.699) for Tokyo can be observed. Afterwards, both economies recover within only two years to nearly the same level as before the crisis.

2.4. Meteorological data

In order to exclude that the results were influenced by meteorological characteristics, the European Center for Medium-Range Weather Forecasts (ECMWF) Reanalysis v5 (ERA-5) data from the Copernicus Climate Change Service (C3S) is analyzed. Further information about the ERA-5 data can be found in Hersbach et al. (2017, 2018, 2020).

With regard to the possible influence of meteorological conditions on the NO_2-pollution during the time periods, A, B, and C we analyzed more closely the hourly ERA-5 data regarding the 2m temperature, the total cloud coverage and wind speed based on the u- and v-component of the wind. The data was downloaded for UTC 1500 (8 a.m. PDT summer time), UTC 1600 (9 a.m. PDT summer time), UTC 1700 (10 a.m. PDT summer time), and UTC 1800 (11 a.m. PDT summer time) for Los Angeles as well as UTC 2300 (8 a.m. JST), UTC 0000 (9 a.m. JST), UTC 0100 (10 a.m. JST), and UTC 0200 (11 a.m. JST) for Tokyo. The mean values of each meteorological parameter as well as area of interest were calculated between 8 a.m. and 11 a.m. (PDT and JST) to cover the overflight time of the satellites. Afterwards, the mean values and the standard deviations (SD) of the different periods A, B, and C, which were derived from the NO_2 variabilities, were calculated to identify changes over time (see Table 1 and Table 2). Furthermore, based on the wind u- and v-component the wind speed is calculated (Table 1).

As Table 1 for the greater Los Angeles area presents, the deviations in terms of windspeed, precipitation as well as temperature between the time periods A, B and C are minor. It is therefore unlikely that meteorology can explain the observed significant decline in NO_2 variability shown in Fig. 8B for the periods B and C.

The same approach as aforementioned was performed for the greater Tokyo area. As presented in Table 2 the average values for the investigated periods A, B, and C show only minor changes and therefore could not be the cause for the significant reduction of NO_2 variability especially for the period B, and C (Fig. 9).

Due to the fact that the satellite observations used in this paper only deliver observations during more or less clear sky conditions, cloud cover only plays a minor in our analysis. Moreover Georgoulias et al. (2019) describe that only data with a cloud radiance fraction of less than 50% - which is equivalent to a cloud fraction with less than 20% - is considered for the data base we use. Furthermore, the authors mention that only data with a surface albedo smaller than 0.3 is used and moreover data with a solar zenith angle higher than 80° is filtered out as well.

The cloud analysis is used to determine the average number of days used in the calculation of the monthly averages regarding the cloud coverage. This is important because the used data product does not contain any information on how many days were considered for the monthly mean values. In order to better understand the cloud cover in the two study areas, we looked at hourly ECMWF ERA-5 data from C3S

about the total cloud cover (see Hersbach et al., 2017, 2018, 2020). Fig. 3 presents the number of days within a month with less than 20% cloud cover. A closer look on the total cloud cover above the greater Los Angeles area reveals that on average 13 days per month are available. Regarding the greater Tokyo area, the ERA-5 data shows that on average 3.5 days per month are obtainable whereas the spline (blue curve) reveals a slightly increasing trend. Moreover, all study areas in Fig. 3 portray an annual cycle. Los Angeles for instance displays on average fewer days with less than 20% total cloud cover in January, whereas Tokyo has fewer days in July. The latter can be explained by the monsoon season in spring.

As shown in Fig. 4A, the mean (blue dot) of the daily total cloud cover for the greater Los Angeles area varies between 46% in February and 21% in August. The most cloud free days occur during the summer months – June, July, August, and September – with a density (Fig. 4A gray shaded area) of the total cloud cover with less than 12% and a median between 16% and 21%. In comparison to that Fig. 4B represents the greater Tokyo area where the highest total cloud cover appears during June and July with a mean value of 79% and 73%. This can be referred due to the monsoon season in spring which is also called "Tsuyu".

3. Methods

The data visualization is done by using the programming language R with the packages "ggplot2" (Wickham, 2016), and "lubridate" (Grolemund and Wickham, 2011; Spinu et al., 2018).

The long-term trend in Fig. 5 is calculated by using the "mgcv" package by Wood (2017). This makes it possible to subtract the long-term trend effects from the NO_2 observations and proceed with the spectral analysis methods described in the following subchapters.

Moreover, the maps of the study areas are made with Natural Earth. The vector and raster map data are freely available and can be downloaded at www.naturalearthdata.com.

3.1. Harmonic analysis

This study employs the methodological approach of harmonic analysis (HA) to subtract seasonal variations (e.g. annual cycle) from the time series. The methodology of HA is a well-established spectral analysis method but a brief description of its formula and scope is warranted. The following description of HA is based on that of Bichler and Bittner (2022) that applies this methodology for a related purpose and to a similar data set type. If the amplitude A_i, the phase φ_i, and the period τ_i with $i = 1, \ldots n$ is known it is possible to model ($y_{mod}(t)$) the original time series $y(t)$ to a certain degree by applying a linear superposition of n sinusoidals.

$$y_{mod}(t) = \sum_{i=1}^{n} A_i \, sin\left(\frac{2\pi}{\tau_i} t + \varphi_i\right) \tag{1}$$

$$\sum_{t=1}^{N} \left[y(t) - y_{mod}(t)\right]^2 \rightarrow 0 \tag{2}$$

As mentioned, the HA in this article is used to extract the annual and

Table 1

Averaged meteorological parameters and standard deviation (SD) for the investigated periods A, B, and C for the greater Los Angeles area in the United States shown in Fig. 8. Source: Hersbach et al. (2017, 2018), Generated using Copernicus Climate Change Service (C3S) Information [2022].

Los Angeles	A		B		C	
	Jan. 97 – Nov. 07		Dec. 07 – Apr. 12		May 12 – Dec. 16	
	Mean	SD	Mean	SD	Mean	SD
Windspeed	1.59 m/s	0.95 m/s	1.69 m/s	1.00 m/s	1.57 m/s	0.90 m/s
Total precipitation	0.03 mm	0.00018 mm	0.03 mm	0.00017 mm	0.02 mm	0.00012 mm
2m temperature	16.89 °C	5.96 °C	15.78 °C	5.98 °C	17.73 °C	5.77 °C

Table 2

Averaged meteorological parameters and standard deviation (SD) for the investigated periods A, B, and C for the greater Tokyo area in Japan shown in Fig. 9. Source Hersbach et al. (2017, 2018), Generated using Copernicus Climate Change Service (C3S) Information [2022].

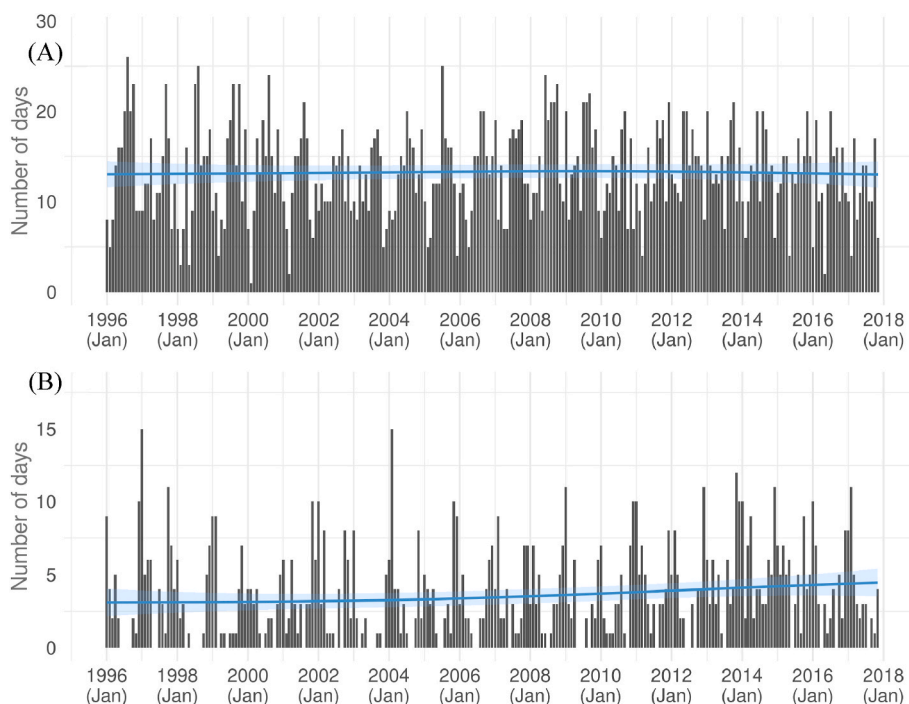| Tokyo | A | | B | | C | |
| | Jan. 97 – Sep. 03 | | Oct. 03 – Jan. 12 | | Feb. 12 – Dec. 16 | |
	Mean	SD	Mean	SD	Mean	SD
windspeed	2.60 m/s	1.48 m/s	2.45 m/s	1.44 m/s	2.47 m/s	1.46 m/s
Total precipitation	0.17 mm	0.00037 mm	0.20 mm	0.00048 mm	0.21 mm	0.0005 mm
2m temperature	14.89 °C	7.84 °C	14.98 °C	7.73 °C	15.57 °C	7.88 °C

Fig. 3. Total cloud cover with less than 20% cloud cover for (A) the greater Los Angeles area and (B) the greater Tokyo area from 1996 to 2017. Source: Hersbach et al. (2017, 2018), Generated using Copernicus Climate Change Service (C3S) Information [2022].

the semi-annual cycle from the tropospheric NO_2 column density time series. To do so, the time series is split into single years starting from July to July of the following year. Afterwards a sinusoidal is fitted to the data based on the least squares method and then subtracted from the data (see equations (1) and (2)). The result are the residues. Equations (1) and (2) can then be applied again on the residues and so on. To further improve the outcoming of the HA the amplitude A_i as well as the phase φ_i are re-fitted to the new time series (residues) at the same time. Further information about the HA and the aforementioned optimization approach can be found in Bittner et al. (1994). As described in Bichler and Bittner (2022) the non-linear system of equations is solved by using the Newton-Raphson method (see Ortega and Rheinboldt, 1970).

3.2. Wavelet analysis

On the other hand, this study also exerts briefly the methodology of the wavelet analysis (WA) to analyze various types of variations such as transient events where an abrupt change takes place, non-stationary signals, local frequency changes such as seasonal patterns as well as non-seasonal variations in the given tropospheric NO_2 time series. In comparison to the HA the WA does not require stationarity in the statistical sense. This means that the time series does not require the same statistical moments such as the standard deviation or the mean values for instance, and therefore not need to be split into single years. This is a great advantage of this method. The wavelet transform can be found in

equation (3). In this equation $f(t)$ represents the given time series, h characterizes the mother wavelet, in this case a *Morlet* wavelet, a is the dilation factor, and b stands for the shift in time.

$$s(a,b) = \frac{1}{\sqrt{a}} \int_{-\infty}^{\infty} f(t) \, h\left[\frac{t-b}{a}\right] dt \tag{3}$$

The *Morlet* wavelet can be described as the following:

$$h(t) = \frac{1}{\pi^{[1/4]}} \left[e^{ikt} - e^{-k^2/2}\right] e^{-t^2/2} \tag{4}$$

where

$$k = \pi \left[\frac{2}{ln\,2}\right]^{1/2} \tag{5}$$

More detailed information on the wavelet transform can be found in Wuest and Bittner (2006), Bittner et al. (2000), Torrence and Compo (1998), as well as Chui (1992).

Within this article the WA is carried out in R by using the "WaveletComp" package from Roesch and Schmidbauer (2018).

4. Results

4.1. NO₂ long-term trend and seasonal variability

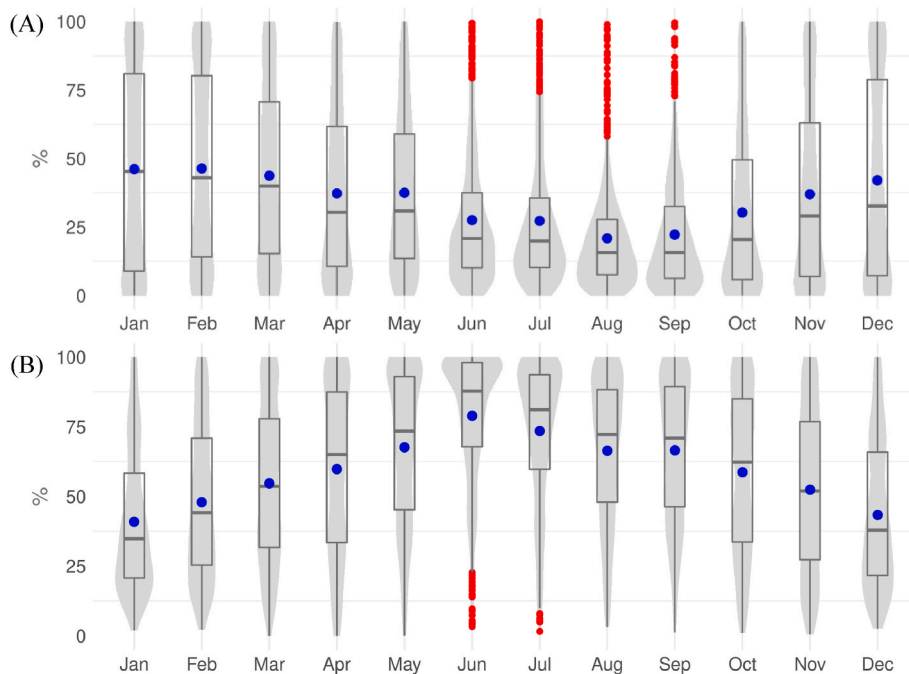The time series of the NO_2 column density for the greater Los Angeles

Fig. 4. Daily total cloud cover for (A) the greater Los Angeles area and (B) the greater Tokyo area divided by months from 1996 to 2017. Gray layer shows the density of the daily total cloud cover over the month. Red dots represent outliers, blue dots indicate the mean value, and the horizontal lines show the median. Source: Hersbach et al. (2017, 2018), Generated using Copernicus Climate Change Service (C3S) Information [2022].
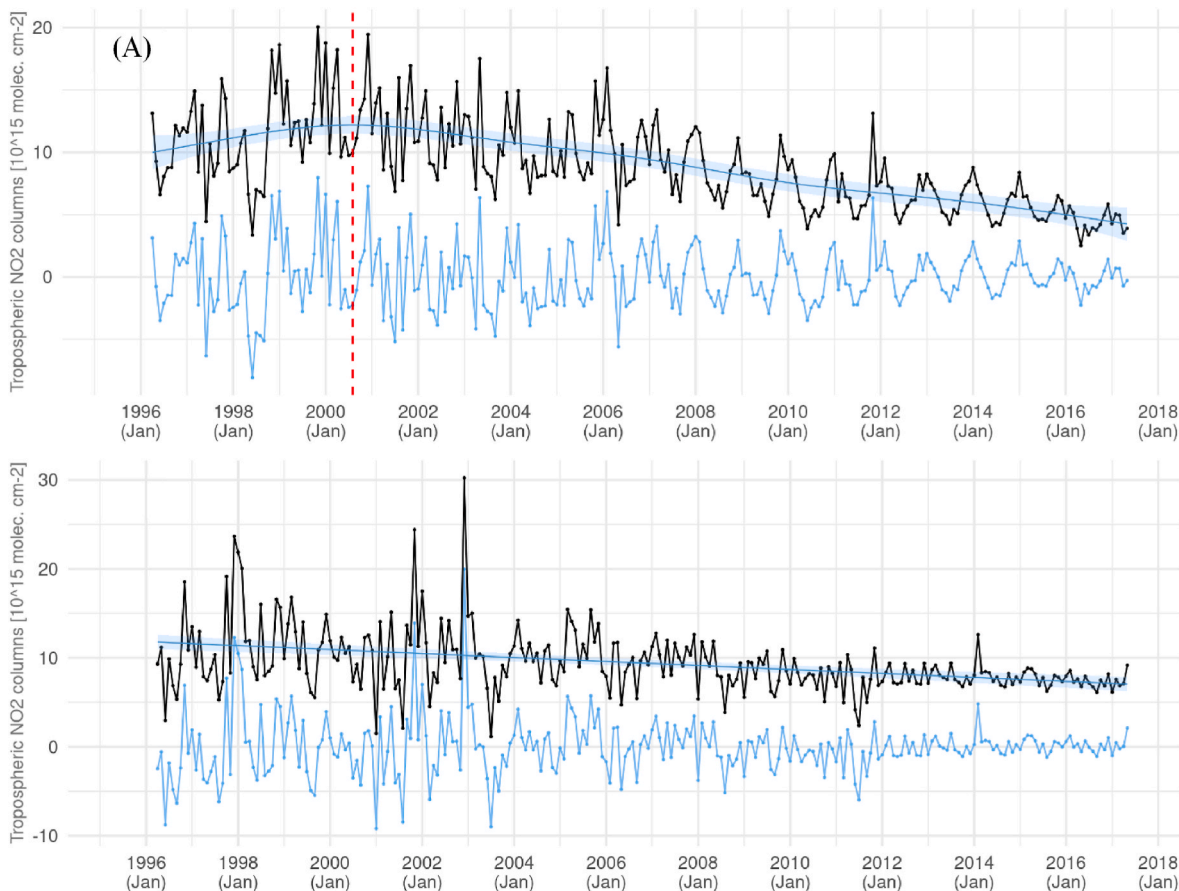

Fig. 5. Time series of the tropospheric NO_2 monthly mean column densities from 1996 to 2017 based on GOME, SICAMCHY, GOME-2A and GOME-2B observations for (A) the area of Los Angeles, California, USA (Latitudes: 33°–35°, Longitudes: 117° − −119°). (B) The area of Tokyo, Japan (Latitudes: 35°–37°, Longitudes: 139° − 141. The black time series shows the original NO_2 observation, the blue time series represents the NO_2 development without the long-term trend, the blue curve represents a cubic spline fit indicating the long-term trend, red line indicates a turning point (see text for detail).

area (Fig. 5A, black curve) shows from 1996 till August 2000 (Fig. 5A red line) an increase in NO$_2$ of about 22% before it then rapidly starts to decrease almost linearly by 64% within the period from August 2000 to 2017. This long-term development is superimposed by shorter scale fluctuations which are shown as the blue curve after taking out the long-term course. Obviously, the strength of these fluctuations decreases with time. The narrowing towards 2017 can be observed by looking at the course of the local maxima and minima. A closer look on the development of the fluctuations also present structural differences for the period from 1996 to 2007 compared to the succeeding period from 2008 to the end of 2017. In fact, it appears that the periodicity of the fluctuations changes with time. While fluctuations on time scales of a few months are strongly characterizing the fluctuations in the years up to about 2006/2007, the annual cycle increasingly emerges thereafter. In order to quantify the temporal development of the annual cycle we performed a harmonic analysis. It turns out that the amplitude of the annual cycle is in the order of about 1–5 * 10^{15} molecules cm^{-2}. They show a clear tendency to decrease over the years as is shown in Fig. 6A. It is also striking that the long-term decrease in the amplitude of the annual cycle is superimposed by a quasi-two-year variation with a peak-to-peak variation in the order of about 1 * 10^{15} molecules cm^{-2}.

Examining the amplitudes, after applying the harmonic analysis for the annual cycle in the study area of Los Angeles, it can be observed that the height of the amplitudes decreases by 53% (Fig. 6A, blue spline).

In contrast, the cubic spline for the greater Tokyo area indicates a continuously decreasing and as a linear incline appearing trend with an overall reduction of about 40% (Fig. 5B, black curve). Like Los Angeles the gray splines show a similar trend of a significant narrowing towards 2017. Regarding to the strength of the fluctuations (blue curve in Fig. 5B), a pronounced reduction can be noticed from 2004 onwards.

The temporal development of the annual cycle is shown in Fig. 6B. The annual cycle strongly weakens in time reaching amplitudes down to about 0.5 * 10^{15} molecules cm^{-2} from 2008 on. Note that the annual cycle also seems to reveal a quasi-two-year modulation.

An even stronger decline in the amplitudes can be detected in the greater Tokyo area where the amplitudes decrease by 96% between 1996 and 2017 (Fig. 6B, blue spline).

4.2. NO$_2$ sub-seasonal variability

The NO$_2$-fluctuations shown in Fig. 5A and B (blue curves) contain contributions also in the sub-seasonal range. In order to quantify them, a wavelet analysis was applied to the time series of the fluctuations. The spectrograms are given in Fig. 7A for Los Angeles and in Fig. 7B for the Tokyo greater area. The panels beside the wavelet-spectrograms give the mean wavelet spectral density averaged separately for each period.

The NO$_2$-fluctuations for Los Angeles are characterized by strong contributions with periods of around 12 months (annual cycle) and contributions with shorter periods and peaking around three months. The latter could indicate the influence of the Madden-Julian oscillation (MJO) (Jones, 2000; Zhou et al., 2020) but further research needs to be done.

The wavelet spectrogram indicates that the annual cycle extends over almost the entire time series. It is consistent what is already said above that the variability of the annual cycle varies over time and reaches comparatively lower values around 2003–2004 and low values from 2016 to 2017. Strikingly noticeable are also strong fluctuation at a period of around three months. Specifically, the years 1997, 2000, 2001, 2003, and 2006 emerge. Starting in 2007 the NO$_2$ – and apart from a short period of increased activity around 2012 - variability decreases
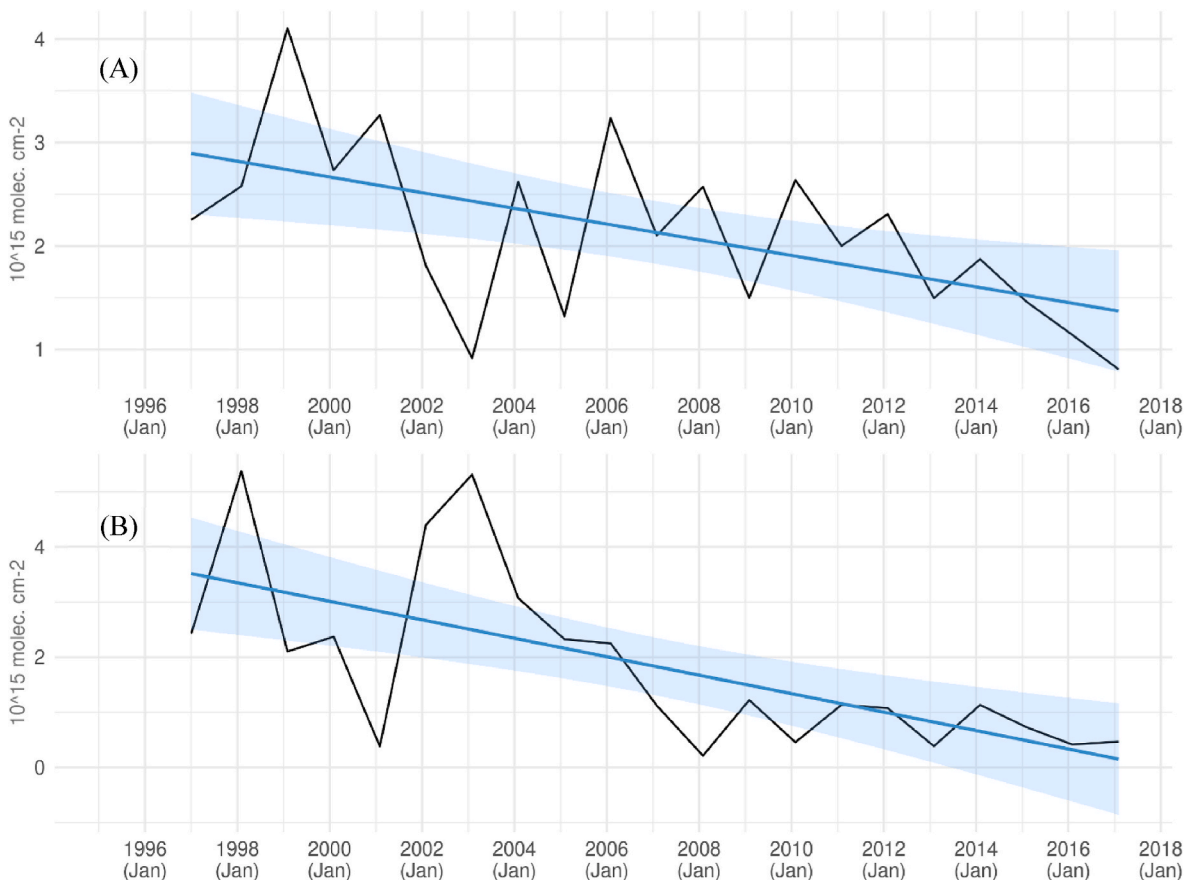

Fig. 6. Development of the amplitude of the annual cycle (black line) in the tropospheric column NO$_2$ - time series between 1996 and 2017 for (A) the greater Los Angeles area and (B) the greater Tokyo area. The blue lines represent a cubic spline to visualize long-term tendencies.
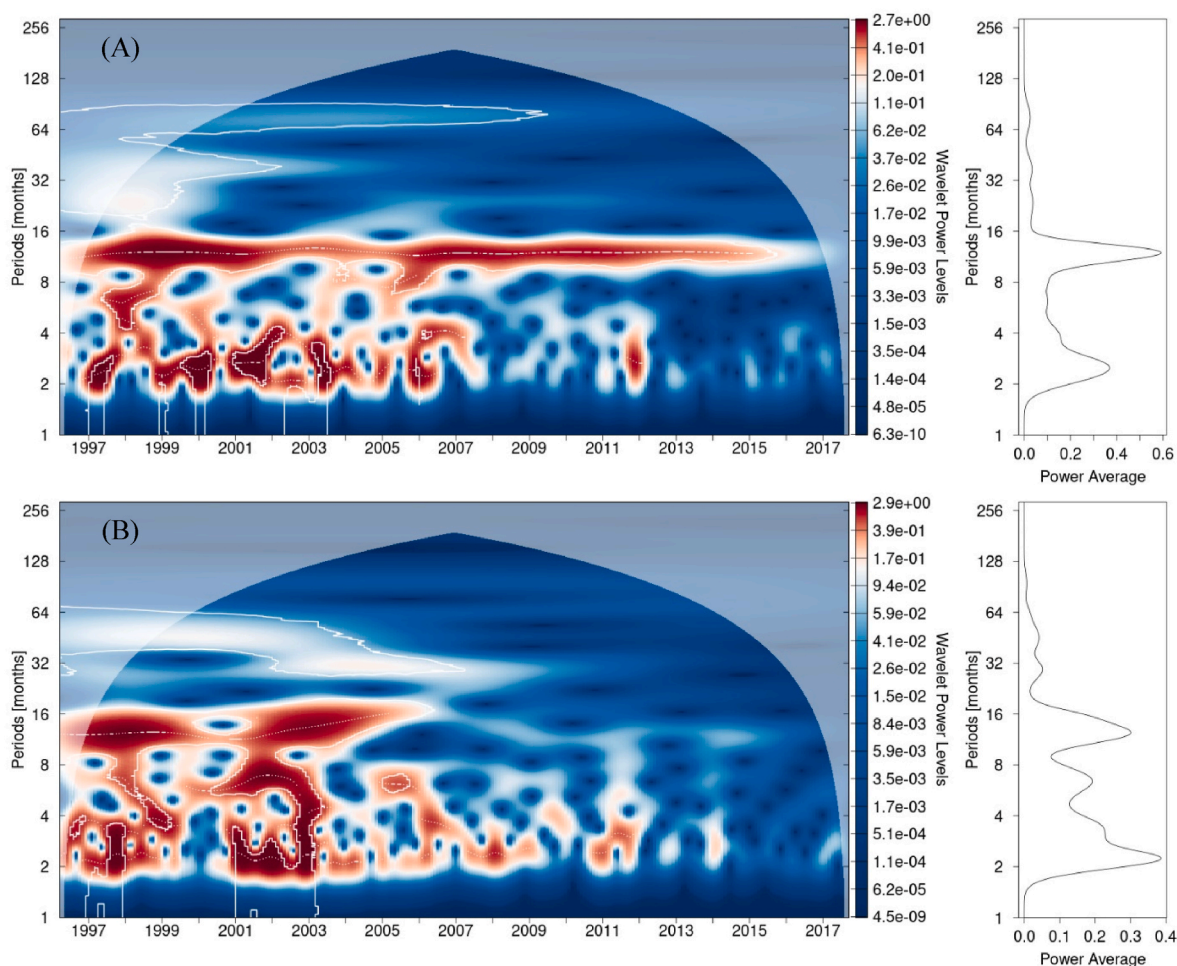
Fig. 7. Wavelet power spectrum based on the residues shown in Fig. 5 for (A) the greater Los Angeles area and (B) the greater Tokyo area. White contours show significant areas, the shaded area reveals the cone of influence which marks areas that might be influenced by edge-effects due to the stretched Morlet wavelet on the edges of the time series, and the plots on the right side represents the related average wavelet power in the frequency domain (averages over time) over the entire period from 1996 to 2017 (Roesch and Schmidbauer, 2018).

significantly in this frequency range and this continues until the end of 2017. Note that there are also enhanced intensities at longer periods. A quasi two-year variation is visible between 1997 and 2007 which could be caused by the quasi-biennial oscillation (QBO). There is also some indication for the presence of variations in the period range of about 40 months as well as 80 months. This could be caused by the time intervals of three (36 months) to seven years (84 months) between two El Niño events which are part of the El Niño-Southern Oscillation (ENSO).

Fig. 7B represents the results of the spectral analysis for the greater area of Tokyo, Japan. Beginning with the plot on the right side, six ranges of periodicities with enhanced amplitudes can be detected. Two maxima are present between the period two and four months which could indicate the Madden-Julian oscillation (MJO), the third maximum arises at a period of around six months which implies the semi-annual cycle. Afterwards another peak can be observed at around twelve months which represents the annual cycle. The last two maxima are noticeable at around 32 months and 48 months. Like Los Angeles the two to four-year signal could be caused by ENSO.

Regarding to the related wavelet-spectrogram, a significant signal is present between the periods of 30 and 64 months. This signal spans from 1996 until 2008. However, for the following nine years, the aforementioned signal cannot be detected anymore. Studying the annual cycle at the period of around 12 months reveals that the variability is stronger between 1996 and 2000, as well as from 2001 to 2006. In between, a significant drop in the fluctuation can be detected in the year 2000.

Remarkably, the annual cycle almost dissolves after 2006. Stronger signals in the NO_2 variability can further be observed in the sub-seasonal frequency region at the end of 1997, in 1999, 2001, 2002, and 2003. Strikingly, the timespan between 2004 and 2012 where a strong decrease of the fluctuations is noticeable over almost the whole frequency range. Moreover, the succeeding period from 2012 to 2017 presents an even stronger significant drop in the NO_2 variability.

In order to get a more precise picture of the sub-seasonal fluctuations, we took out the longer-term signals, the annual and semi-annual cycles from the original time series by means of the harmonic analysis. The residues for the greater Los Angeles area are shown in Fig. 8A (blue line) are then subject to the wavelet analysis. The resulting wavelet spectrogram is shown in Fig. 8B. This adjusted wavelet spectrogram clearly shows that the sub-seasonal variability strongly decreases from 2008 onwards with an exception in 2012.

Based on the wavelet-spectrogram shown in Fig. 8B we identified three time zones with different spectral characteristics as shown by the squares A, B, and C. By calculating the monthly mean wavelet intensity values between the periods of two (according to the Nyquist-Shannon criterion) and six months, it is possible to quantify the change of the sub-seasonal NO_2 variability between the identified time zones A, B, and C. From time zone A to time zone B we find a reduction in NO_2 variability of around 77%. A further reduction from time zone B to time zone C leads to a decrease by 82%.

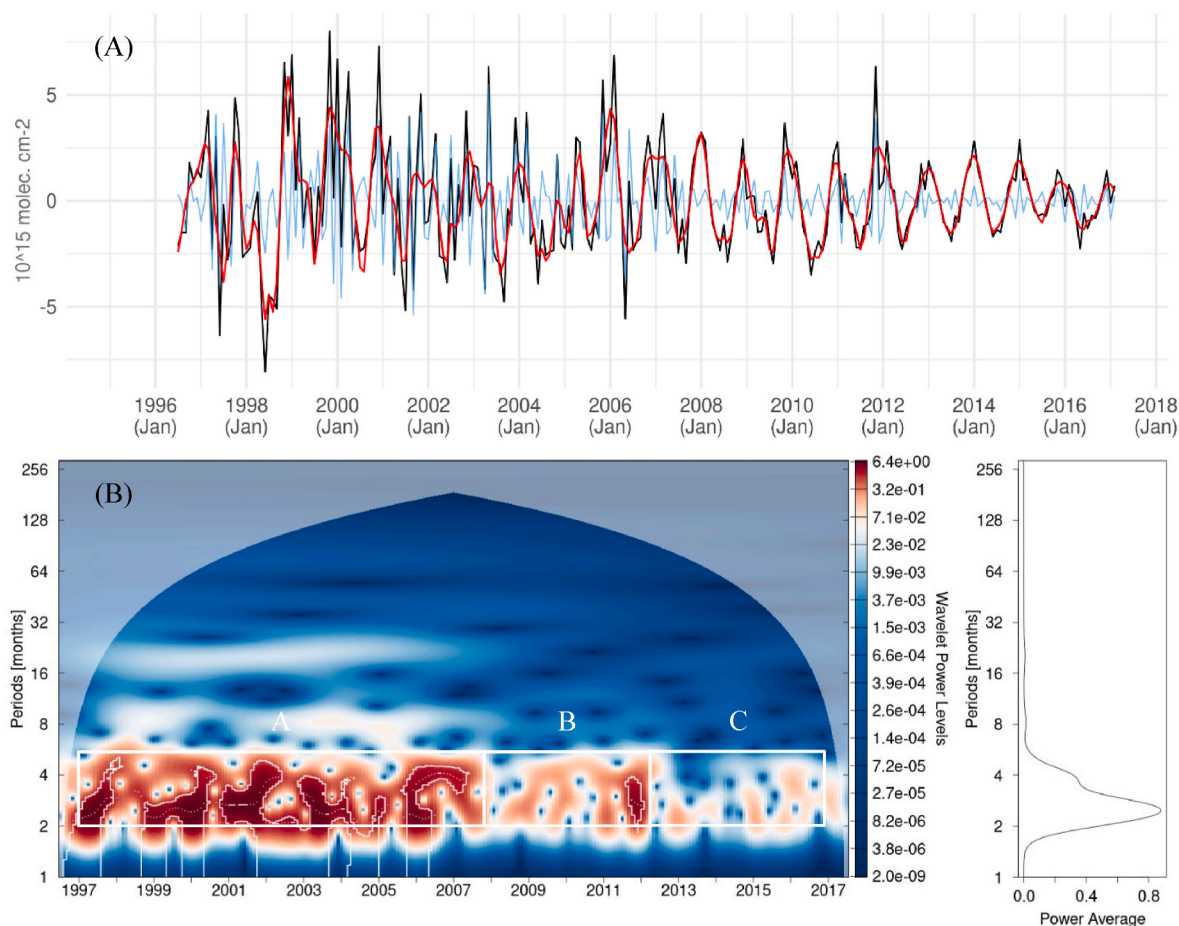Fig. 9 gives the results for the greater area of Tokyo. The NO_2-

Fig. 8. Spectral analysis results for the greater Los Angeles area. (A) Harmonic analysis fit based on the annual and semi-annual cycles presented as red curve. The black curve shows the original time series with subtracted long-term trend. The blue curve visualizes the residues which is the result of subtracting the red curve from the black curve. (B) Wavelet spectrogram for the residues shown in Fig. 8A (blue curve).

fluctuations adjusted for the annual and half-year cycle (blue curve in Fig. 9A) show significantly lower values from about 2004 than in the previous period. This is also reflected in the wavelet spectrogram. The variability of the intensities of the sub-seasonal fluctuations can be divided into three time zones, A, B, and C (see Fig. 9B). We tentatively did not designate the drop in intensity in 2000 as a separate time zone. Again, the sub-seasonal NO_2 variability was estimated for each time zone separately by averaging the wavelet intensities between the periods two and six months. We find a decrease in NO_2 variability of around 73% from time zone A to time zone B. A reduction of around 80% is found from time zone B to time zone C.

5. Discussion

5.1. NO_2 long-term trend

The long-term NO_2 development for the greater Los Angeles (Fig. 5A) systematically increases from 1996 to August 2000 by about 22% before it reaches a turning point. From there on the NO_2 pollution appears to decrease almost linearly by about 64%. Superimposed is a seasonal variation showing higher NO_2 values in winter times and lower values during summer times. The amplitude is found to decrease over time by about 53% (Fig. 6A).

There are several studies which address the long-term trend of air quality in the Los Angeles region. For example, Brioude et al. (2013) studied air pollution measurements taken during several NOAA (National Oceanic and Atmospheric Administration) P-3 aircraft campaigns in combination with three different transport models. The main goal of

Brioude et al. (2013) was to evaluate and improve the National Emission Inventory (NEI) 2005, however, one of the results that fits the content of our paper is that the posterior NO_y ($NO_y = NO_x + PAN + HNO_3 + NO_3^-$) emissions for the Los Angeles County decreased by 36% ± 10% and 37% ± 15% for the South Coast Air Basin (SoCAB) between 2002 and 2010. This reduction in NO_x emissions is in line with our finding. We derive a reduction of tropospheric NO_2 of around 39.8% between 2002 and the end of 2010.

Russell et al. (2012) analyzed OMI data, they report about a decrease in NO_2 of 40.3% for Los Angeles from 2005 to 2011. The authors conclude that the results indicate that improved emission control technology for on-road mobile sources led to a reduction in NO_2 pollution. Hassler et al. (2016) who analyzed the inventory NO_x emissions find a decrease by 45.3% ± 10.9% between 2005 and 2014. They conclude that NO_x emissions declined due to more stringent vehicle emission standards as well as the growing importance of heavy-duty diesel engines. And Duncan et al. (2016) found a reduction in satellite-based observations of the NO_2 tropospheric column based on OMI/Aura data over Los Angeles of around 56.4% ± 5.6% between 2005 and 2014. Duncan et al. (2016) conclude for various cities in the U.S., Europe, and Japan that the changes in NO_2 pollution might be caused due to local, regional, and/or country specific environmental regulations. Moreover, a study by Tong et al. (2015) reviled a reduction in NO_x over Los Angeles by around 40% based on OMI data and a 37% based on ground observations (Air Quality System, AQS) between 2005 and 2012. Regarding to the authors this is probably caused by combined effects of emission control regulations as well as the economic recession. The findings of Tong et al. (2015) compare quite well with our result which gives a
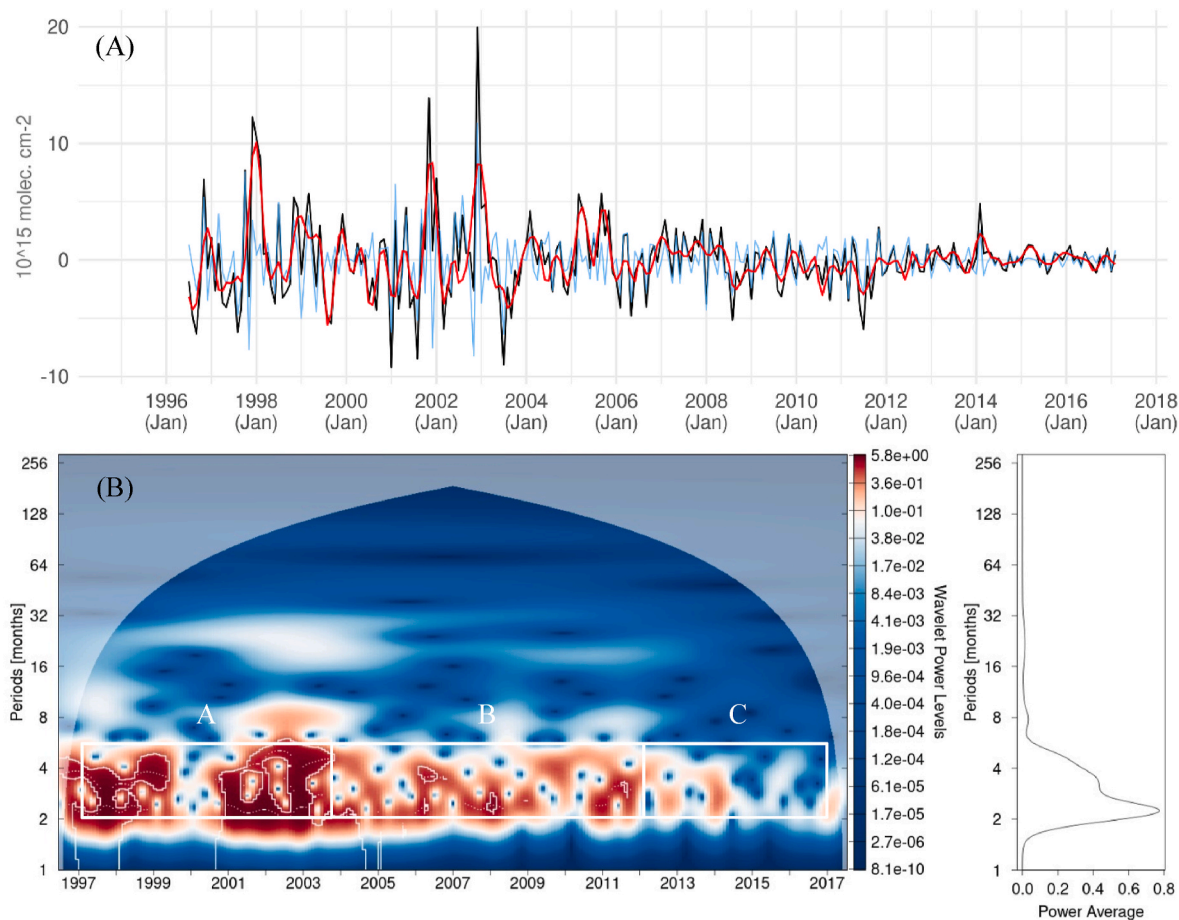
Fig. 9. Spectral analysis results for the greater Tokyo area. (A) Harmonic analysis fit based on the annual and semi-annual cycle presented as red curve. The black curve shows the original time series with subtracted long-term trend. The blue curve visualizes the residues which is the result of subtracting the red curve from the black curve. (B) Wavelet spectrogram for the residues shown in Fig. 9A (blue curve).

reduction of the tropospheric NO_2 column densities of about 42% from 2005 to the end of 2014.

Additionally, Hassler et al. (2016) found a decreasing NO_x/CO pollution after 2007 in their fuel-based inventory data. The authors reference this event with the global economic crisis which had an impact on freight traffic. This further led to a decrease in NO_x emissions for the Los Angeles Basin by around 41%.

In the greater Tokyo region, there are also several studies available which address the long-term change of air quality. For example, Duncan et al. (2016) also find a decrease in the NO_2 column density for Tokyo of around $38.3 \pm 8.3\%$ between 2005 and 2014. The authors indicate that local, regional, and/or country specific environmental regulations led to the large NO_x decrease in Tokyo for instance. However, Duncan et al. (2016) mention that western parts of Japan experience weaker changes in NO_x pollution. Regarding to the authors this might be caused due to transboundary NO_x pollution from China. Additionally, Choo et al. (2020) analyzed the tropospheric NO_2 VCD from Aura/OMI data from 2005 to 2018. The authors describe that the VCD for Japan decreased by $3.55 \pm 2.37 * 10^{15}$ molecules cm^{-2}. In comparison to that, the decrease of the linear trend between 2005 and 2017 based for the Tokyo area in our studies is about $2.74 * 10^{15}$ molecules cm^{-2} which equals a reduction of around 28%.

Moreover, Choo et al. (2020) mention a decrease in the tropospheric NO_2 VCD for Japan of around 30% between 2005 and 2017. In comparison to that, the long-term NO_2 tropospheric column densities (Fig. 5B) in our studies decreases almost linearly over the whole period (1996–2017) by 40%. It can be said, that those results are very similar, although it must be pointed out that we analyzed a longer period of time,

a smaller study area as well as NO_2 observations in the morning not around noon. Nevertheless, Choo et al. (2020) concludes that the NO_2 trends over Northeast Asia might be caused by various socio-economic changes such as economic growth/recession, environmental policy and so forth.

In our study we show that the long-term trend is superimposed by smaller scale fluctuations in a scale of a few months. By removing the long-term decrease from the NO_2 time series, we find that the variations between 2004 and 2017 are significantly smaller than from 1996 to 2004. In other words, the amplitudes are significantly smaller during the period from 2004 to 2017 in comparison to the previous years. In general, the height of the amplitudes decreased by about 96% (Fig. 6B).

Souri et al. (2017) also examined OMI NO_2 data and found for Japan a downward trend in the yearly averaged time series for all three study periods from 2005 to 2014 ($-0.06 * 10^{15}$ molecules cm^{-2} yr^{-1}), 2005 to 2010 ($-0.11 * 10^{15}$ molecules cm^{-2} yr^{-1}), and 2010 to 2014 ($-0.03 * 10^{15}$ molecules cm^{-2} yr^{-1}). The authors imply that this is a result of strictly persistent air pollution regulations. However, Souri et al. (2017) also mention that other parts of Japan might be influenced by the export of Chinese NO_x emissions.

Based on the results, it should be mentioned that the selected study areas seem to be quite successful in their ongoing decoupling of economic activity from air pollution.

It should be noted at this point that, based on literature as well as reports from the United States Environmental Protection Agency (EPA), the long-term decline of NO_2 pollution (Fig. 5) for both study areas seem to be a result of air pollution control measures.

In the greater Los Angeles region, the EPA introduced the Clean Air

Act in the 1990s. Since then, the exhaust gas emission standards got stricter and the fuel composition environmental friendlier (EPA, 2022). Stringent standards for emissions caused by diesel engines during construction, agriculture, industrial equipment or marine applications were applied. In 1999, based on EPA reports the emission standards for cars were also applied for the first time to light-duty trucks as well as sport utility vehicles (SUVs) (EPA, 2022). Additionally, large marine diesel engines were forced to reduce their NO_x and PM emissions which may have led to further reductions in air pollution (EPA, 2022). In 2000, a new regulation for nonroad handheld engines such as chainsaws or bush cutters etc. came into effect which also led to a reduction of hydrocarbons (HC) and NO_x pollution. A national control program was also developed to regulate 2007 model year heavy-duty vehicles as well as the inherent fuel. Between 2001 and 2016 EPA further established the Clean School Bus USA program, stricter standards for nonroad diesel

engines, marine diesel engines as well as motorcycles. Additionally, the Smart Way Transportation Partnership program was introduced and changes for commercial aircraft engines regarding their NO_x emissions were made. Due to the Energy Policy Act from 2005 the Renewable Fuel Standard Program as well as the Diesel Emission Reduction Program were established. A stringent emission standard was also adopted for locomotives regarding to their PM and NO_x pollution. EPA also notes that due to the 2007 Energy Independence and Security Act the composition of fuel changed by adding 15% of ethanol to the mixture, also known as E15. Furthermore, the Emission Control Area (ECA) for shared waters by the US, Canada, and France was developed (EPA, 2022).

In addition to the California Ambient Air Quality Standards (CAAQP), another reason for the long-term decline in NO_2 pollution for Los Angeles could be the implementation of the low-emission vehicle
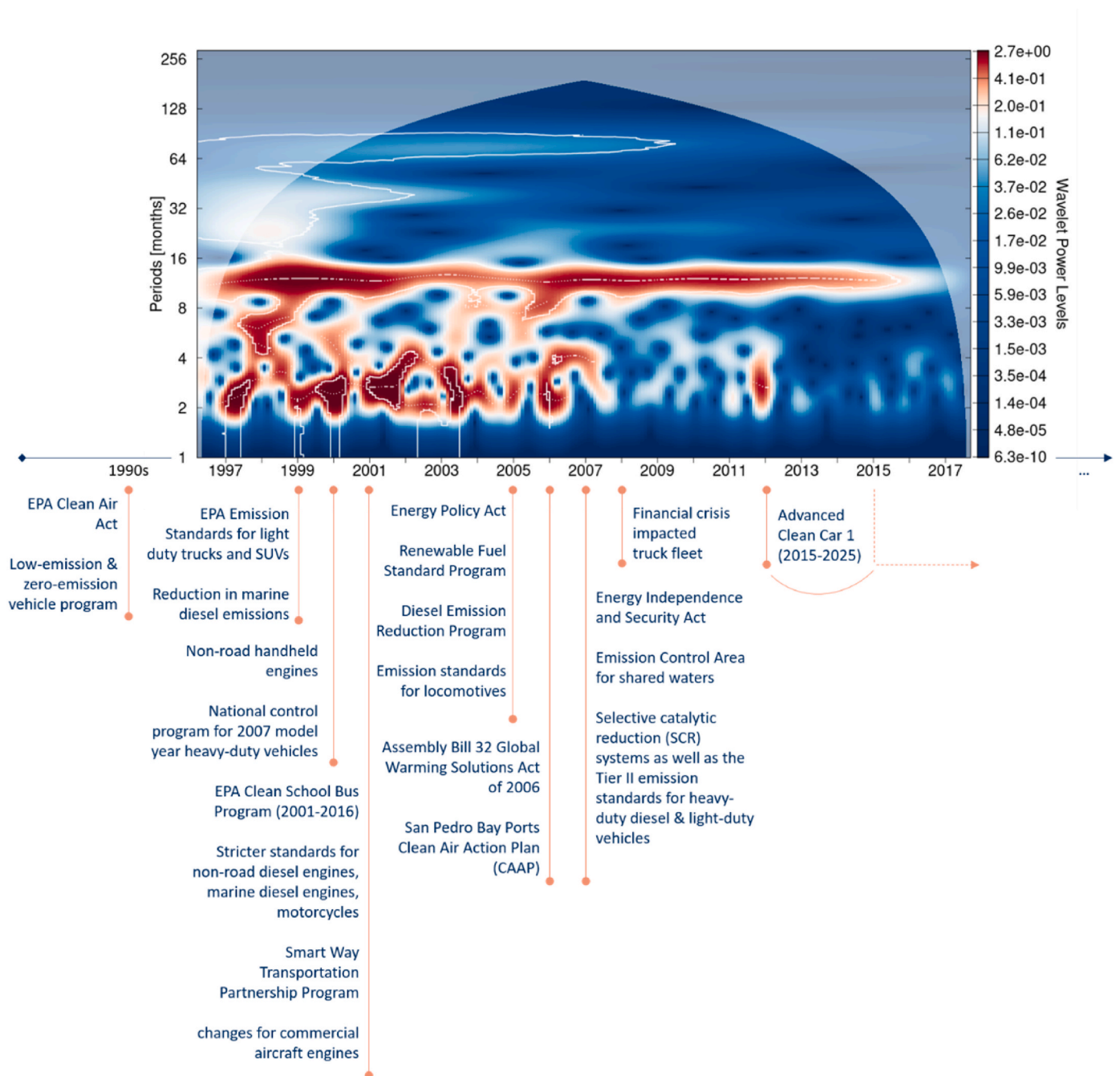

Fig. 10. Comparison of the wavelet spectrogram with political air pollution control measures for the study area in Los Angeles.

(LEV) and zero-emission vehicle (ZEV) program in 1990 (CARB, 2022, 2022a, 2022b). Both programs, LEV and ZEV, were later combined in the California's Advanced Clean Cars Program. The Advanced Clean Car (ACC) I regulation was introduced in 2012 to regulate the period between 2015 and 2025 and will be followed by the ACC II regulation for the period 2026 to 2035. The goal of the ACC II is that by 2035 all new passenger vehicles, trucks, as well as SUVs that will be sold in the state of California shall be zero emission vehicles (CARB, 2022c). California also established the Assembly Bill 32 Global Warming Solutions Act of 2006 to reduce greenhouse gas (GHG) emissions. Since GHGs as well as NO_2 pollution has its source mostly by fossil fuel combustion, thus regulations for GHGs can have an impact on air pollutants as well. Within the literature Hassler et al. (2016), Bishop et al. (2015), McDonald et al. (2012, 2013), and Bishop and Stedman (2015) further mention the implementation of NO_x emission control technologies such as the selective catalytic reduction (SCR) systems as well as the Tier II emission standards which lead to a reduction in air pollution for heavy-duty diesel vehicles as well as light-duty vehicles after 2007. Also, worth mentioning is the impact of the global financial crisis in 2008 on the truck fleet population. Due to the recession, emissions from diesel as well as gasoline trucks decreased largely (Bishop and Stedman, 2015; Hassler et al., 2016).

Furthermore, in 2006 the San Pedro Bay Ports Clean Air Action Plan (CAAP) was introduced. This plan was created and established between the Port of Los Angeles and Long Beach with the task to reduce port emissions (Giuliano and Linder, 2013; CAAP, 2017, 2017a). Giuliano and Linder (2013) also stress out that ports are complex in terms of their *"fragmented regulations"* due to international trade. Therefore, emissions can be regulated for instance by federal, state or local agencies (Giuliano and Linder, 2013). Nevertheless, referring to the authors the CAAP is an example of self-regulation which was adopted because of *"the loss of social legitimacy, to social pressure that were restricting the ability of the ports to expand, and to regulatory threats"*. Although the authors further conclude that at least 50% of air pollution was reduced by the CAAP in comparison to without the initiative.

In a direct comparison with the wavelet spectrogram (Fig. 10), the Energy Policy Act, the Renewable Fuel Standard Program, and the Diesel Emission Reduction Program stand out. All three measures are established in 2005 and if a start-up period of one and a half year is considered, significant drops in NO_2 variability can be observed. Moreover, the Assembly Bill 32 Global Warming Solutions Act, as well as the San Pedro Bay Ports CAAP in 2006 show similar results after less than one year. Additionally, in 2007 the SCR systems, the Tier II emission standards, as well as the Energy Independence and Security Act also seem to have a positive impact on the reduction of the NO_2 variability. From 2015 onwards, it can also be seen that the annual cycle loses intensity which is probably supported by the ACC 1.

Like California, Japan has taken environmental protection measures early on such as the Air Pollution Control Act in 1968 (Act No. 97 of June 10, 1968). Nevertheless, in this paper we aimed to address measures that became effective in the period between 1996 and 2017 and therefore might influenced the NO_2 variability in Tokyo. As Hara et al. (2013) emphasizes, the Ministry of Land, Infrastructure, Transport, and Tourism (MILT) established several national laws to reduce air pollution. Regarding Hara et al. (2013), in the years 1994, 1997, 2003, 2005, and 2009 the diesel vehicle exhaust emission standards from brand-new cars continuously became stricter. Furthermore, in 2002 the Automobile NO_x and PM Control law was introduced which especially had an impact on the use of older vehicles (Hara et al., 2013; TransportPolicy.net, 2018; DieselNet, 2015). Within their study, Hara et al. (2013) concluded that the traffic volume especially of diesel trucks decreased in Tokyo and might be the effect of stricter regulations but also due to technological improvements regarding the engine. The authors found a reduction in $PM_{2.5}$ of 49.8% between 2001 and 2010. Furthermore, Japan is since 2012 a partner of the Climate and Clean Air Coalition (CCAC) which not only focuses on the reduction of GHG but also air pollution (CCAC,

2022). Additionally, Japan introduced the Feed-In Tariff (FIT) in 2012 in order to promote renewable energy (METI, 2017).

On sub-national level, the Tokyo Metropolitan Government (TMG) established a new Ordinance on Environmental Preservation at the end of 2000. This regulation included the Countermeasure Against Vehicle Pollution program which consist of six different strategies and came into effect in October 2003 (Hara et al., 2013; ESCI Energy Smart Communities Initiative, 2014; TransportPolicy.net, 2018a; DieselNet, 2015a). Also, from 2002 to 2005 the Tokyo Carbon Reduction Reporting Program for existing large facilities was introduced (EBRD, 2023). This was a mandatory reporting scheme that helped identify one's potential to reduce the energy consumption. This initiative and the outcome of several meetings with various stakeholders paved the way for the cap-and-trade program (Roppongi et al., 2017; TMG, 2023). The TMG introduced the cap-and-trade program in 2010, which was proposed in the Tokyo Climate Change Strategy of 2007 to regulate GHG emissions within a five-year period. Like Roppongi et al. (2017) notes, Tokyo's cap-and-trade program was worldwide the first city-scale scheme that also included the regulation of buildings to reduce GHG emissions. The authors further stress that Tokyo was able to reduce 23% of GHG emissions after 2013 compared to the base years. This was done by regulating energy consumers such as large building facilities for example. As the name of the program indicates, the exceeding emission can be capped through five different types of credits. If there is no improvement regarding to the emissions, the Governor of Tokyo can issue a warning to the specific facility and, in worst case, impose a fine of up to 500.000JP¥ (Roppongi et al., 2017). This regulation not only reduces GHG, but also trace gases, as these are also associated with energy consumption. Additionally, the Tokyo Carbon Reduction Reporting for Small and Medium Entities (CRR) Program is a mandatory reporting initiative for CO_2 emissions that was launched in 2010 (EBRD, 2023; TMG, 2018; TMG, 2018a; TMG, 2018b). Moreover, TMG announced in 2019 the Zero Emission Tokyo Strategy, which aims to achieve net zero CO_2 emissions by 2050 (TMG, 2019; TMG, 2019a). Since CO_2 is also produced as a product of fossil fuel combustion, this strategy also has a positive impact on reducing air pollutants.

Similar results are found for Tokyo. In this regard, the Automobile NO_x PM Control law as well as the Tokyo Carbon Reduction Program which were introduced in 2002 appear to have had an impact on the NO_2 variability one year later. Furthermore, in 2003 the diesel vehicle exhaust emission standards for brand-new cars became stricter and in addition the Countermeasure Against Vehicle Pollution program came into effect while at the same time the wavelet spectrogram (Fig. 11) shows significant declines in NO_2 variability. Starting in 2005 the annual cycle loses substantial on intensity and disappears completely after 2006. A further decrease in smaller fluctuations between the periods of two and eight can also be seen in 2009. At both points in time, 2005 and 2009, measures for diesel vehicle exhaust emission standards for brand-new cars tightened again. In 2010 the five-year period for the cap-and-trade program was introduced and the wavelet analysis shows once more a striking reduction in NO_2 variability.

Both wavelet spectrograms in Figs. 10 and 11 suggest that the air pollution control measures mentioned resulted in a reduction of NO_2 pollution and variability. Detailed research on pollution measures as well as pollution variability can help identify effective measures and apply them to other study regions to promote better air quality.

5.2. NO_2 seasonal and sub-seasonal variability

To better understand the NO_2 variability based on smaller scale fluctuations, the wavelet analysis (Figs. 7, Fig. 8, and Fig. 9) will be discussed. The wavelet spectrogram for the study area in Los Angeles (Fig. 7A) presents a strong annual cycle at a 12 months period due to temperature differences between summer and winter. After deducting the annual cycle from the NO_2 time series (Fig. 8) variations in smaller scales come out more clearly.
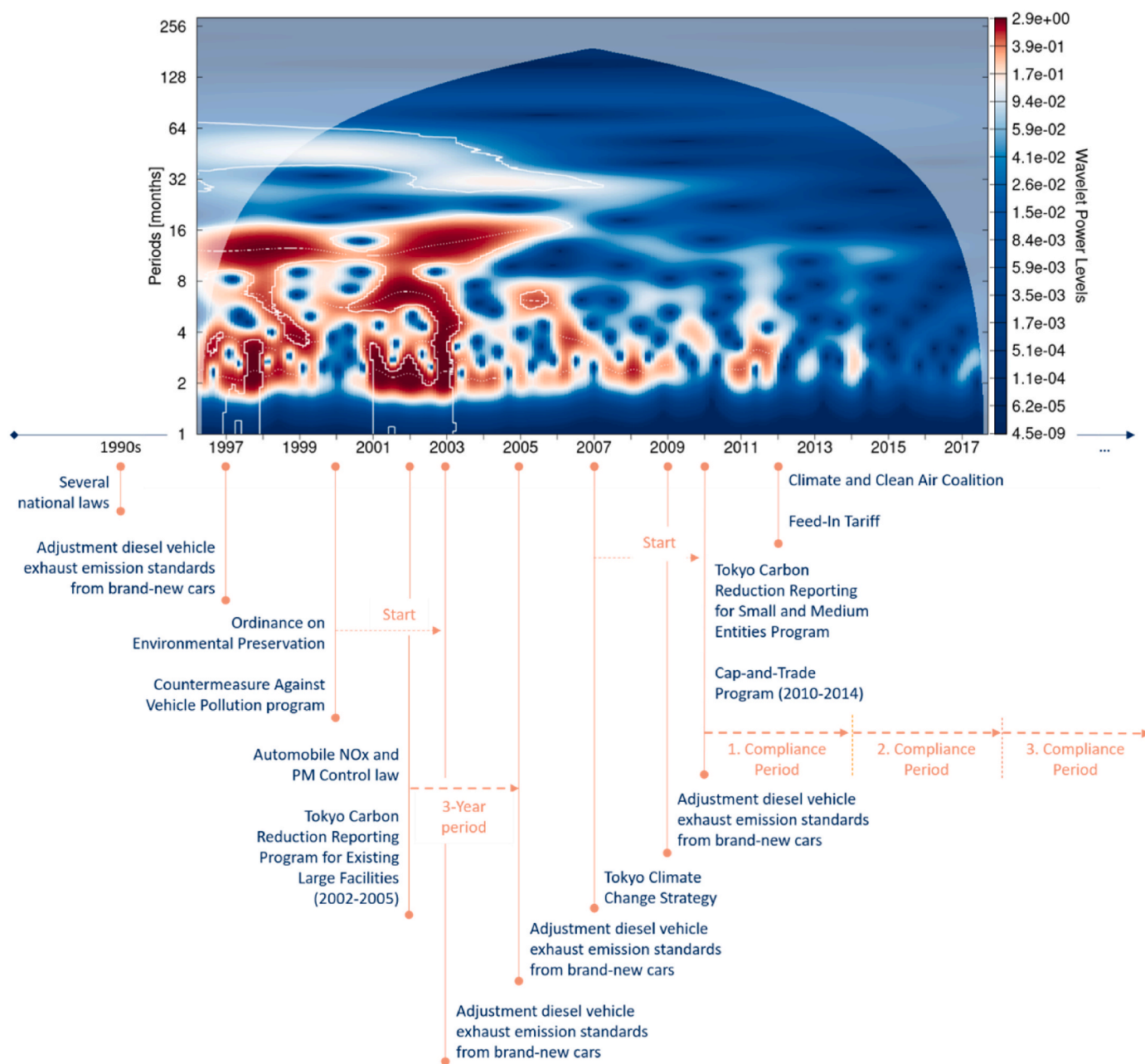
Fig. 11. Comparison of the wavelet spectrogram with political air pollution control measures for the study area in Tokyo.

It should also be mentioned that the study area in Los Angeles (Fig. 7A) shows a significant section between the periods 64 and 96, which is indicated by a white bordered line. This signal implies a five to eight-year cycle, which could be caused by the El Niño-Southern Oscillation (ENSO). Additionally, the amplitudes in Fig. 6A of Los Angeles present a maximum almost every two years, which could imply the quasi-biennial oscillation (QBO). This is a phenomenon in the stratosphere in which the wind directions change at a cyclic interval. Moreover, the QBO can be observed worldwide.

Regarding sub-seasonal fluctuations in a range of a few months a strong decrease in the variability can be observed strikingly well in the period starting from 2007 to 2017. In contrast, in the previous period (Figs. 5A and 1996–2007) there are a few years in which the variability is significantly more distinct. A reduction of the variability in the subsequent period could be caused on the one hand by short-term events such as the global financial crisis in 2007/2008. Bichler and Bittner (2022), and references therein, further point out the low-periodic NO_2

fluctuations are mostly a composition of production, loss, and transport processes. This can be written as

$$\frac{\partial NO_2}{\partial t} = P_i - L_j - u\vec{\Delta}NO_2 \qquad (6)$$

where t is the time, u is the velocity, $\vec{\Delta}$ is the three-dimensional spatial gradient operator, P is the production, and L stands for the loss on NO_2, i and j intended to represent different processes. On the other hand, changes that reduce smaller variabilities and thus lead to a clearer appearing of the annual cycle (Figs. 5A and 2007–2017) may have been brought as a result of aforementioned persistent political measures to improve air quality.

McDonald et al. (2012, 2013) emphasize that on-road vehicles are the dominant source (around 80%) for anthropogenic NO_x emission in Los Angeles. They further describe that between 2007 and 2009 the two study areas – the Los Angeles basin and the San Joaquin Valley – observe

a decrease of around 10% per year in NO_x. The authors suspect the connection with the economic crisis which had an impact on the freight sector and further mention that the sales regarding to diesel fuel fell by 13%–17% whereas gasoline dropped by 2%–6%. Furthermore, Russell et al. (2012) found a reduction in NO_2 column densities for Los Angeles prior (2005–2007), during (2007–2009), and after (2009–2011) the global economic crisis of around 5.47%, 14.99%, and 2.15% per year.

It is now possible to quantify the reduction of the NO_2 variability based on three periods A, B, and C. As described in the literature, the periods A, B, and C can also be divided into before, during, and after the economic crisis. When dividing the economic development into the same three periods as shown in Fig. 8 it can be observed that the NO_2 pollution during period A (1997 to end of 2007) is more pronounced than in subsequent years. At the same time, the GDP development between 2001 and 2007/2008 is constantly rising. Subsequently, the second phase starting at the end of 2007 presents a slight decline in economic output, triggered by the global economic crisis. However, until the beginning of 2012 the economy is able to recover and reaches before crisis levels again. In comparison, there is a significant decrease in NO_2 variability during this crisis-ridden phase. During the second period there is a 77% decrease in NO_2 variability compared to the previous time. Although, within period C, ranging from the beginning of 2012–2017, the economic output starts to increase again whereas NO_2 pollution continues to fall, is very interesting. Compared to period B, NO_2 variability decreased by another 82% in period C. The drifting apart of GDP development and NO_2 pollution can be interpreted as decoupling process.

In Tokyo (Fig. 7B), an annual cycle can be found from 1996 to 2005/2006. Afterwards the variability of the annual cycle becomes hardly noticeable in the spectrogram. Additionally, the wavelet spectrogram shows a significant area between the periods 32 and 64 which indicates an almost three to five-year cycle. The amplitudes of the study area for Tokyo (Fig. 6B) also show higher values almost every two years. This phenomenon could also be caused by the aforementioned QBO. Also, the smaller scale fluctuations decrease significantly beginning in mid-2003. When subtracting the long-term trend from the NO_2 time series (Fig. 9) the decrease in NO_2 variability can be divided into three periods.

From period A to period B a reduction of around 73% and from period B to period C a reduction of around 80% of NO_2 variability can be observed. Looking at the economic output it can be noticed that a decoupling between the NO_2 pollution and the GDP development started already in 2003. From there on the NO_2 variability significantly decreases especially for fluctuations between period two and period eight which can be seen in Fig. 7B and in Fig. 9B. It is also astonishing that the annual cycle from 2007 onwards ends abruptly (Fig. 7B). At the same time, the GDP has shown significant slumps since 2007, which only recovered in 2012 where the economic output is back at a pre-crisis level. It can now be speculated to what extent the economic crisis has affected the NO_2 annual cycle. What is certain, however, is that even after 2012 annual cycle is not appearing again and the decoupling process continues.

In some study areas, transboundary air pollution can also occur due to special wind flow conditions and adjacent sources of pollution. Takashima et al. (2011) analyzed the NO_2 pollution observed by MAX-DOAS observations over Cape Hedo on the Okinawa Island in Japan by applying backward trajectory calculations on meteorological data. They found that the NO_2 pollution was higher when strong westerly winds occurred due to a low-pressure system over Japan. In those cases, polluted air masses were transported from the east coast of central China. This means that higher variabilities can arise for a short time (~24h) due to transport processes in the marine boundary layer. Similar research regarding the transportation of anthropogenic air pollutants from East Asia to Cape Hedo, Okinawa in Japan was also carried out by Hatakeyama et al. (2011) where the authors also concluded that within the transportation of air mass photochemical oxidation reactions took place. Moreover, Kajino et al. (2013) analyzed the total deposition of

nitrate (TDN) for 2006 and additionally conducted a source-receptor relationship (SRR) analysis for March, July, and December 2006. Within the study the authors concluded that Chinese emissions contributed around 50%–60% of the TDN in South Korea and Japan. As Choo et al. (2020) and OECD (2016) emphasize, transboundary air pollution has become a serious social, economic as well as a diplomatic issue especially for countries close to significant air pollution sources. In this study, transboundary influences were not examined in detail due to the temporal resolution of the satellite observations for the area of interest in Tokyo. Therefore, it is not possible to make a statement about the extent to which such transboundary air pollution processes have influenced our results but provide potential for future research. Moreover, Irie et al. (2016) and Souri et al. (2017) for instance also mention the impact on the NO_2 pollution by the Fukushima Daiichi nuclear power plant accident due to a tsunami which was caused by a massive earthquake close to the Pacific coast in 2011. Both authors describe that more energy was generated in the power plant sector after the accident which lead to an increase in NO_2 column densities. The findings of Irie et al. (2016) who found an increase of around 13% per year in the NO_2 VCD from 2013 to 2015 based on OMI data cannot be confirmed. Nevertheless, the slightly higher NO_2 variability between a period of two to 12 months in 2011 shown in Fig. 7B might be a result of the nuclear power plant damage; however, further investigation is needed.

6. Summary and conclusion

In this study, we used a self-consistent tropospheric NO_2 VCD time series based on GOME, SCIAMACHY, and GOME-2 with a temporal resolution of monthly mean values which covers a period from 1996 to 2017 from Georgoulias et al. (2019). In a further step the satellite observations are studied by using two spectral analysis methods – the harmonic analysis as well as the wavelet analysis. This approach makes it possible to observe the temporal development of the NO_2 variability in a certain area. Since NO_2 can be influenced by meteorological conditions, the possible impact of precipitation, wind, and temperature is analyzed. It is determined that the meteorology had no significant influence on our results. This study identified successful examples, Tokyo and Los Angeles, of a decoupling process between NO_2 pollution and economic activity using spectral analysis methods based on satellite observations.

The main conclusions of this study are:

1. Decoupling process between NO_2 pollution and GDP growth

Both study areas show a decoupling process of NO_2 pollution and GDP development. This occurs when NO_2 pollution decreases over time while the GDP increases. It can thus be assumed that the economy in these study areas has developed in a sustainable manner. From the study area in Los Angeles, this can be observed from 2008 onwards (Fig. 7A), with a strong annual cycle remaining due to seasonal changes. However, minor fluctuations between the periods two through eight months decrease significantly, while the economy recovers and grows after the global financial crisis in 2008 (Fig. 2A). In comparison to that the NO_2 variability in Tokyo significantly decreases starting in 2004 (Fig. 7B). Remarkable about the study area is also the disappearance of the annual cycle in the spectrogram which means that Tokyo has managed to integrate air pollution measures that completely remove NO_2 pollution caused by seasonal changes. Referring to the economy it is shown in Fig. 2B that from 2002 to 2007 a strong GDP growth is taking place. Between 2007 and 2009 Tokyo suffers from the impacts of the financial crisis but in 2011, the city returned to pre-financial crisis levels.

2. Air pollution control measures

The influence of political air pollution control measures is particularly evident when examining the long-term trend (Fig. 5). For the

greater Los Angeles area, a constantly and almost linear declining NO_2 trend can be observed starting in the year 2000 (Fig. 5A). Moreover, after 2008 shorter scale fluctuations disappear, which can be recognized by a clearer appearance of the annual cycle. These developments can be traced back to several initiatives of EPA on a national scale as well as air pollution control measures such as the CAAQP, LEV regulations, ZEV regulations, SCR systems, as well as the CAAP for instance on a sub-national scale. Tokyo, on the other hand, shows a linear decline in NO_2 pollution from the start in 1996 (Fig. 5B). These developments might be ascribed to steadily tightened diesel vehicle exhaust emission standards, the Automobile NO_x PM Control law, the introduced Ordinance on Environmental Preservation which includes the Countermeasure Against Vehicle Pollution program, as well as the Tokyo Carbon Reduction Reporting program that led to the cap-and-trade program, for example.

This study has shown that the NO_2 variabilities can provide an indication of whether economic activities are developing more sustainably and whether goals such as those in the UN SDGs or the European Green Deal for instance can be achieved or not. Based on satellite observations, these targets can thus be observed worldwide. Nevertheless, because we only focus on NO_2 pollution there is room for further research on other air pollutants. Another limitation of this paper is that we only focus on the GDP as a whole, therefore, a more detailed analysis regarding the different economic sectors would offer potential.

Further studies could cities that successfully implement air quality measures and continue to grow their GDP, such as Los Angeles and Tokyo. Furthermore, an investigation on why some air pollution control measures are more effective than others would have high potential for future studies. The resulting findings could then be implemented in political measures in other countries to improve air quality. In other words, effective measures from other countries could be identified and established in other study areas. The extent to which the outsourcing of industries, foreign trade, consumer spending or population development for instance has an impact on air pollution was not examined in this study, but would show potential for future investigations in other areas around the world.

CRediT authorship contribution statement

Renée Bichler: Conceptualization, Writing – original draft, Writing – review & editing, Data curation, Methodology, Software, programming, Formal analysis, Visualization. **Stefan Samuel Schönebeck:** Writing – original draft, Formal analysis. **Michael Bittner:** Writing – original draft, Writing – review & editing, Supervision.

Declaration of competing interest

The authors declare that they have no known competing financial interests or personal relationships that could have appeared to influence the work reported in this paper.

Data availability

All datasets are freely available and have been provided with a corresponding link in the paper.

Acknowledgement

References

Al Yammahi, A., Aung, Z., 2022. A study of nitrogen dioxide (NO_2) periodicity over the United Arab Emirates using wavelet analysis. Sci. Rep. 12, 18144 https://doi.org/10.1038/s41598-022-21937-3.

Beirle, S., Borger, C., Dörner, S., Li, A., Hu, Z., Liu, F., Wang, Y., Wagner, T., 2019. Pinpointing nitrogen oxide emissions from space. Sci. Adv. 5 (11), eaax9800 https://doi.org/10.1126/sciadv.aax9800.

Bichler, R., Bittner, M., 2022. Comparison between economic growth and satellite-based measurements of NO_2 pollution over northern Italy. Atmos. Environ. 272, 118948 https://doi.org/10.1016/j.atmosenv.2022.118948.

Bishop, G.A., Stedman, D.H., 2015. Reactive nitrogen species emission trends in three light-/medium-duty United States fleets. Environ. Sci. Technol. 49 (18), 11234–11240. https://doi.org/10.1021/acs.est.5b02392.

Bishop, G.A., Hottor-Raguindin, R., Stedman, D.H., McClintock, P., Theobald, E., Johnson, J.D., Lee, D.-W., Zietsman, J., Misra, C., 2015. On-road heavy-duty vehicle emissions monitoring system. Environ. Sci. Technol. 49 (3), 1639–1645. https://doi.org/10.1021/es505534e.

Bittner, M., Offermann, D., Bugaeva, I.V., Kokin, G.A., Koshelkov, J.P., Krivolutsky, A., Tarasenko, D.A., Gil-Ojeda, M., Hauchecorne, A., Lübken, F.-J., de la Morena, B.A., Mourier, A., Nakane, H., Oyama, K.I., Schmidlin, F.J., Soule, I., Thomas, L., Tsuda, T., 1994. Long period/large scale oscilllations of temperature during the DYANA campaign. J. Atmos. Terr. Phys. 56, 1675–1700. https://doi.org/10.1016/0021-9169(94)90004-3.

Bittner, M., Offermann, D., Graef, H.H., 2000. Mesopause temperature variability above a midlatitude station in Europe. J. Geophys. Res. 105 (D2), 2045–2058. https://doi.org/10.1029/1999JD900307.

Boersma, K.F., Jacob, D.J., Eskes, H.J., Pinder, R.W., Wang, J., 2008. Intercomparison of SCIAMACHY and OMI tropospheric NO_2 columns: observing the diurnal evolution of chemistry and emissions from space. J. Geophys. Res. 113, D16S26. https://doi.org/10.1029/2007JD008816.

Bovensmann, H., Burrows, J.P., Buchwitz, M., Frerick, J., Noel, S., Rozanov, V.V., Chance, K.V., Goede, A.H.P., 1999. Sciamachy – mission objectives and measurement modes. J. Atmos. Sci. 56, 127–150. https://doi.org/10.1175/1520-0469(1999)056%3c0127:SMOAMM%3e2.0.CO;2.

Brasseur, G.P., Jacob, D.J., 2017. Modeling of Atmospheric Chemistry. Cambridge University Press, ISBN 978-1-107-14696-9.

Brioude, J., Angevine, W.M., Ahmadov, R., Kim, S.-W., Evan, S., McKeen, S.A., Hsie, E.-Y., Frost, G.J., Neuman, J.A., Pollack, I.B., Peischl, J., Ryerson, T.B., Holloway, J., Brown, S.S., Nowak, J.B., Roberts, J.M., Wofsy, S.C., Santoni, G.W., Oda, T., Trainer, M., 2013. Top-down estimate of surface flux in the Los Angeles Basin using a mesoscale inverse modeling technique: assessing anthropogenic emissions of CO, NO_x and CO_2 and their impacts. Atmos. Chem. Phys. 13, 3661–3677. https://doi.org/10.5194/acp-13-3661-2013.

Burrows, J.P., Hoelzle, E., Goede, A., Visser, H., Fricke, W., 1995. Sciamachy – scanning imaging absorption spectrometer for atmospheric chartography. Acta Astronaut. 35, 445–451. https://doi.org/10.1016/0094-5765(94)00278-T.

Burrows, J.P., Weber, M., Buchwitz, M., Rozanov, V., Ladstaetter-Weissenmayer, A., Richter, A., Debeek, R., Hoogen, R., Bramstedt, K., Eichmann, K.-U., Eisinger, M., Perner, D., 1999. The global ozone monitoring exeriment (GOME): mission concept and first scientific results. J. Atmos. Sci. 56, 151–175. https://doi.org/10.1175/1520-0469(1999)056<0151:TGOMEG>2.0.CO;2.

CAAP (Clean Air Action Plan), 2017. San Pedro Bay Ports Clean Air Action Plan 2017 Draft Final. Online: https://kentico.portoflosangeles.org/getmedia/9d371f7b-9812-4c75-bcfd-23e83a191435/CAAP_2017_Draft_Document-Final. (Accessed 3 November 2022).

CAAP (Clean Air Action Plan), 2017a. San Pedro Bay Ports Clean Air Action Plan. Factsheet 2017. Online: https://kentico.portoflosangeles.org/getmedia/d082e8ae-8d30-4f65-8dee-cb3c4a31f8d3/CAAP_2017_Factsheet_7_12_17. (Accessed 3 November 2022).

CARB (California Air Resources Board), 2022. California Ambient Air Quality Standards. Online: https://ww2.arb.ca.gov/resources/california-ambient-air-quality-standards. (Accessed 4 November 2022).

CARB (California Air Resources Board), 2022a. Low-emission vehicle program. Online: https://ww2.arb.ca.gov/our-work/programs/low-emission-vehicle-program/about. (Accessed 3 November 2022).

CARB (California Air Resources Board), 2022b. Zero-emission vehicle program. Online: https://ww2.arb.ca.gov/our-work/programs/zero-emission-vehicle-program/about. (Accessed 3 November 2022).

CARB (California Air Resources Board), 2022c. Advanced clean cars program. Online: https://ww2.arb.ca.gov/our-work/programs/advanced-clean-cars-program. (Accessed 3 November 2022).

Castellanos, P., Boersma, K.F., 2012. Reduction in nitrogen oxides over Europe driven by environmental policy and economic recession. Sci. Rep. 2, 265. https://doi.org/10.1038/srep00265.

CCAC (Climate and Clean Air Coalition), 2022. Japan. CCAC partner since 2012. About. Online: https://www.ccacoalition.org/en/partners/japan. (Accessed 3 November 2022).

Choo, G.-H., Seo, J., Yoon, J., Kim, D.-R., Lee, D.-W., 2020. Analysis of long-term (2005-2018) trends in tropospheric NO$_2$ percentiles over Northeast Asia. Atmos. Pollut. Res. 11, 1429–1440. https://doi.org/10.1016/j.apr.2020.05.012.

Chui, C.K., 1992. An introduction to wavelets. Math. Comput. 60 (202), 854. https://doi.org/10.2307/2153134.

Cui, Y., Zha, H., Dang, Y., Qiu, L., He, Q., Jiang, L., 2022. Spatio-temporal heterogeneous impacts of the drivers of NO$_2$ pollution in Chinese cities: based on satellite observation data. Rem. Sens. 14 (14), 3487. https://doi.org/10.3390/rs14143487.

DieselNet, 2015. Emission standards. Japan: Tokyo retrofit program. Online: https://dieselnet.com/standards/jp/tokyofit.php. (Accessed 3 March 2023).

DieselNet, 2015a. Emission Standards. Japan. Automotive NO$_x$ and PM Law. Online: https://dieselnet.com/standards/jp/noxpmlaw.php. (Accessed 3 March 2023).

Dinda, S., Coondoo, D., Pal, M., 2000. Air quality and economic growth: an empirical study. Ecol. Econ. 34 (3), 409–423. https://doi.org/10.1016/S0921-8009(00)00179-8.

Duncan, B.N., Lamsal, L.N., Thompson, A.M., Yoshida, Y., Lu, Z., Streets, D.G., Hurwitz, M.M., Pickering, K.E., 2016. A space-based, high-resolution view of notable changes in urban NOx pollution around the world (2005–2014). J. Geophys. Res. Atmos. 121, 976–996. https://doi.org/10.1002/2015JD024121.

Earth, Natural, 2023. Populated Places. City and Town Points, from Tokyo to Wasilla, Cairo to Kandahar. Online:, Version 5.1.2. https://www.naturalearthdata.com/downloads/10m-cultural-vectors/10m-populated-places/. (Accessed 3 March 2023).

EBRD (European Bank for Reconstruction and Development), 2023. The Green Cities Policy Tool. Carbon Reduction Reporting Programme: Tokyo, Japan. Online: https://www.ebrdgreencities.com/policy-tool/carbon-reduction-reporting-programme-tokyo-japan-2/#context-and-policy-overview. (Accessed 3 March 2023).

Epa (United States Environmental Protection Agency), 2022. Timeline of Major Accomplishments in Transportation, Air Pollution, and Climate Change. Online: https://www.epa.gov/transportation-air-pollution-and-climate-change/timeline-major-accomplishments-transportation-air. (Accessed 16 November 2022).

ESCI (Energy Smart Communities Initiative), 2014. ST-1.1 energy-efficient vehicles. Tokyo vehicle emissions reduction retrofit program. Online: https://www.esci-ksp.org/archives/project/tokyo-vehicle-emissions-reduction-retrofit-program?task_id=593. (Accessed 3 March 2023).

Eskes, H.J., Boersma, K.F., 2003. Averaging kernels for DOAS total-column satellite retrievals. Atmos. Chem. Phys. 3, 1285–1291. https://doi.org/10.5194/acp-3-1285-2003.

Fang, D., Yu, B., 2021. Driving mechanism and decoupling effect of PM2.5 emissions: empirical evidence from China's industrial sector. Energy Pol. 149, 112017 https://doi.org/10.1016/j.enpol.2020.112017.

Filonchyk, M., Peterson, M., 2020. Air quality changes in shanghai, China, and the surrounding urban agglomeration during the COVID-19 lockdown. J. Geovis. Spat. Anal. 4, 22. https://doi.org/10.1007/s41651-020-00064-5.

Filonchyk, M., Hurynovich, V., Yan, H., 2021. Impact of COVID-19 pandemic on air pollution in Poland based on surface measurements and satellite data. Aerosol Air Qual. Res. 21, 200472 https://doi.org/10.4209/aaqr.200472.

Geddes, J.A., Martin, R.V., Boys, B.L., van Donkelaar, A., 2016. Long-term trends worldwide in ambient NO2 concentrations inferred from satellite observations. Environ. Health Perspect. 124, 281–289. https://doi.org/10.1289/ehp.1409567.

Georgoulias, A.K., vander, A., R, Stammes, P., Boersma, K.F., Eskes, H.J., 2019. Trends and trend reversal detection in 2 decades of tropospheric NO$_2$ satellite observations. Atmos. Chem. Phys. 19, 6269–6294. https://doi.org/10.5194/acp-19-6269-2019.

Giuliano, G., Linder, A., 2013. Motivations for self-regulation: the clean air action plan. Energy Pol. 59, 513–522. https://doi.org/10.1016/j.enpol.2013.04.007.

Goldberg, D.L., Anenberg, S.C., Griffin, D., McLinden, C.A., Lu, Z., Streets, D.G., 2020. Disentangling the impact of the COVID-19 lockdowns on urban NO$_2$ from natural variability. Geophys. Res. Lett. 47, e2020GL089269 https://doi.org/10.1029/2020GL089269.

Grolemund, G., Wickham, H., 2011. Dates and times made easy with lubridate. J. Stat. Software 40 (3), 1–25. https://doi.org/10.18637/jss.v040.i03.

Grossman, G.M., Krueger, A.B., 1995. Economic growth and the environment. Q. J. Econ. 110 (2), 353–377. https://doi.org/10.2307/2118443.

GSHHG (Global Self-consistent, Hierarchical, High-resolution Geography Database), 2017. NOAA. Shoreline/Coastline Resources. Data Version 2.3.7. Online: https://www.ngdc.noaa.gov/mgg/shorelines/. (Accessed 3 March 2023).

Hara, K., Homma, J., Tamura, K., Inoue, M., Karita, K., Yano, E., 2013. Decreasing trends of suspended particulate matter and PM2.5 concentrations in Tokyo, 1990-210. J. Air Waste Manag. Assoc. 63 (6), 737–748. https://do-i.org/10.1080/10962247.2013.782372.

Hassler, B., McDonald, B.C., Frost, G.J., Borbon, A., Carslaw, D.C., Civerolo, K., Granier, C., Monks, P.S., Monks, S., Parrish, D.D., Pollack, I.B., Rosenlof, K.H., Reyerson, T.B., von Schneidemesser, E., Trainer, M., 2016. Analysis of long-term observations of NO$_x$ and CO in megacities and application to constraining emissions inventories. Geophys. Res. Lett. 43, 9920–9930. https://doi.org/10.1002/2016GL069894.

Hatakeyama, S., Hanaoka, S., Ikeda, K., Watanabe, I., Arakaki, T., Sadanaga, Y., Bandow, H., Kato, S., Kajii, Y., Sato, K., Shimizu, A., Takami, A., 2011. Aerial observation of aerosols transported from East Asia – chemical composition of aerosols and layered structure of an air mass over the east China sea. Aerosol Air Qual. Res. 11, 497–507. https://doi.org/10.4209/aaqr.2011.06.0076.

Hersbach, H., Bell, B., Berrisford, P., Hirahara, S., Horányi, A., Muñoz-Sabater, J., Nicolas, J., Peubey, C., Radu, R., Schepers, D., Simmons, A., Soci, C., Abdalla, S.,

Abellan, X., Balsamo, G., Bechtold, P., Biavati, G., Bidlot, J., Bonavita, M., De Chiara, G., Dahlgren, P., Dee, D., Diamantakis, M., Dragani, R., Flemming, J., Forbes, R., Fuentes, M., Geer, A., Haimberger, L., Healy, S., Hogan, R.J., Hólm, E., Janisková, M., Keeley, S., Laloyaux, P., Lopez, P., Lupu, C., Radnoti, G., de Rosnay, P., Rozum, I., Vamborg, F., Villaume, S., Thépaut, J.-N., 2017. Complete ERA5 from 1979: fifth generation of ECMWF atmospheric reanalyses of the global climate. Copernicus Climate Change Service (C3S) Data Store (CDS). (Accessed 20 June 2021).

Hersbach, H., Bell, B., Berrisford, P., Biavati, G., Horányi, A., Muñoz Sabater, J., Nicolas, J., Peubey, C., Radu, R., Rozum, I., Schepers, D., Simmons, A., Soci, C., Dee, D., Thépaut, J.-N., 2018. ERA5 hourly data on single levels from 1959 to present. Copernicus Climate Change Service (C3S) Climate Data Store (CDS). https://doi.org/10.24381/cds.adbb2d47. (Accessed 23 November 2022).

Hersbach, H., Bell, B., Berrisford, P., Hirahara, S., Horányi, A., Muñoz-Sabater, J., Nicolas, J., Peubey, C., Radu, R., Schepers, D., Simmons, A., Soci, C., Abdalla, S., Abellan, X., Balsamo, G., Bechtold, P., Biavati, G., Bidlot, J., Bonavita, M., De Chiara, G., Dahlgren, P., Dee, D., Diamantakis, M., Dragani, R., Flemming, J., Forbes, R., Fuentes, M., Geer, A., Haimberger, L., Healy, S., Hogan, R.J., Hólm, E., Janisková, M., Keeley, S., Laloyaux, P., Lopez, P., Lupu, C., Radnoti, G., de Rosnay, P., Rozum, I., Vamborg, F., Villaume, S., Thépaut, J.-N., 2020. The ERA5 global reanalysis. Q. J. R. Meteorol. Soc. 146, 1999–2049. https://doi.org/10.1002/qj.3803.

Hilboll, A., Richter, A., Burrows, J.P., 2013. Long-term changes of tropospheric NO$_2$ over megacities derived from multiple satellite instruments. Atmos. Chem. Phys. 13, 4145–4169. https://doi.org/10.5194/acp-13-4145-2013.

Irie, H., Muto, T., Itahashi, S., Kurokawa, J., Uno, I., 2016. Turnaround of tropospheric nitrogen dioxide pollution trends in China, Japan, and South Korea. SOLA 12, 170–174. https://doi.org/10.2151/sola.2016-035.

Itoh, Y., Kobayashi, M., Okamoto, T., Imaya, A., Sakai, Y., Yoshinaga, S., 2021. Influence of chronic and excessive nitrogen influx on forest ecosystems connected to the Tokyo metropolitan area. Ecol. Indicat. 127, 107771 https://doi.org/10.1016/j.ecolind.2021.107771.

Jia, J., You, Y., Yang, S., Shang, Q., 2022. Analysis of the effect of economic development on air quality in jiangsu province using satellite Remote sensing and statistical modeling. Atmosphere 13 (5), 697. https://doi.org/10.3390/atmos13050697.

Jiang, M., Kim, E., Woo, Y., 2020. The relationship between economic growth and air pollution – a regional comparison between China and South Korea. Int. J. Environ. Res. Publ. Health 17, 2761. https://doi.org/10.3390/ijerph17082761.

Jones, C., 2000. Occurrence of extreme precipitation events in California and relationships with the madden-julian oscillation. J. Clim. 13, 3576–3587. https://doi.org/10.1175/1520-0442(2000)013%3C3576:OOEPEI%3E2.0.CO;2.

Jury, M.R., 2020. Meteorology of air pollution in Los Angeles. Atmos. Pollut. Res. 11 (7), 1226–1237. https://doi.org/10.1016/j.apr.2020.04.016.

Kajino, M., Sato, K., Inomata, Y., Ueda, H., 2013. Source-receptor relationships of nitrate in Northeast Asia and influence of sea salt on the long-range transport of nitrate. Atmos. Environ. 79, 67–78. https://doi.org/10.1016/j.atmosenv.2013.06.024.

Konduracka, E., Rostoff, P., 2022. Links between chronic exposure to outdoor air pollution and cardiovascular diseases: a review. Environ. Chem. Lett. 20, 2971–2988. https://doi.org/10.1007/s10311-022-01450-9.

Le Quéré, C., Jackson, R.B., Jones, M.W., Smith, A.J.P., Abernethy, S., Andrew, R.M., De-Gol, A.J., Willis, D.R., Shan, Y., Canadell, J.G., Friedlingstein, P., Creutzig, F., Peters, G.P., 2020. Temporary reduction in daily global CO$_2$ emissions during the COVID-19 forced confinement. Nat. Clim. Change 10, 647–653. https://doi.org/10.1038/s41558-020-0797-x.

Lelieveld, J., Beirle, S., Hörmann, C., Stenchikov, G., Wagner, T., 2015. Abrupt recent trend changes in atmospheric nitrogen dioxide over the Middle East. Sci. Adv. 1 (7) https://doi.org/10.1126/sciadv.1500498.

Levy II, H., Moxim, W.J., Klonecki, A.A., Kasibhatla, P.S., 1999. Simulated tropospheric NOx: its evaluation, global distribution and individual source contributions. J. Geophys. Res. Atmos. 104 (D21), 26279–26306. https://doi.org/10.1029/1999JD900442.

Li, J., Hou, L., Wang, L., Tang, L., 2021. Decoupling analysis between economic growth and air pollution in key regions of air pollution control in China. Sustainability 13 (12), 6600. https://doi.org/10.3390/su13126600.

Liu, F., Beirle, S., Zhang, Q., Dörner, S., He, K., Wagner, T., 2016. NOx lifetimes and emissions of cities and power plants in polluted background estimated by satellite observations. Atmos. Chem. Phys. 16, 5283–5298. https://doi.org/10.5194/acp-16-5283-2016.

Liu, F., Page, A., Strode, S.A., Yoshida, Y., Choi, S., Zheng, B., Lamsal, L.N., Li, C., Krotkov, N.A., Eskes, H., van der A, R., Veefkind, P., Levelt, P.F., Hauser, O.P., Joiner, J., 2020. Abrupt decline in tropospheric nitrogen dioxide over China after the outbreak of COVID-19. Sci. Adv. 6 (28) https://doi.org/10.1126/sciadv.abc2992.

Liu, S., Valks, P., Beirle, S., Loyola, D.G., 2021. Nitrogen dioxide decline and rebound observed by GOME-2 and TROPOMI during COVID-19 pandemic. Air Qual. Atmos. Health 14, 1737–1755. https://doi.org/10.1007/s11869-021-01046-2.

McDonald, B.C., Dallmann, T.R., Martin, E.W., Harley, R.A., 2012. Long-term trends in nitrogen oxide emissions from motor vehicles at national, state, and air basin scales. J. Geophys. Res. 117, D00V18. https://doi.org/10.1029/2012JD018304.

McDonald, B.C., Gentner, D.R., Goldstein, A.H., Harley, R.A., 2013. Long-term trends in motor vehicle emissions in U.S. urban areas. Environ. Sci. Technol. 47 (17), 10022–10031. https://doi.org/10.1021/es401034z.

METI (Ministry of Economy, Trade and Industry), 2017. Present status and promotion measures for the introduction of renewable energy in Japan. Online: https://www.meti.go.jp/english/policy/energy_environment/renewable/index.html. (Accessed 14 November 2022).

Müller, I., Erbertseder, T., Taubenböck, H., 2022. Tropospheric NO$_2$: explorative analyses of spatial variability and impact factors. Remote Sens. Environ. 270, 112839 https://doi.org/10.1016/j.rse.2021.112839.

Munro, R., Lang, R., Klaes, D., Poli, G., Retscher, C., Lindstrot, R., Huckle, R., Lacan, A., Grzegorski, M., Holdak, A., Kokhanovsky, A., Livschitz, J., Eisinger, M., 2016. The GOME-2 instrument on the Metop series of satellites: instrument design, calibration, and level 1 data processing – an overview. Atmos. Meas. Tech. 9, 1279–1301. https://doi.org/10.5194/amt-9-1279-2016.

net, TransportPolicy, 2018. Japan: emissions: NO$_x$ and PM law. Online: https://www.transportpolicy.net/standard/japan-emissions-nox-and-pm-law/. (Accessed 3 March 2023).

net, TransportPolicy, 2018a. Japan: emissions: Tokyo retrofit. Online: https://www.transportpolicy.net/standard/japan-emissions-tokyo-retrofit/. (Accessed 3 March 2023).

OECD (Organization for Economic Cooperation and Development), 2016. The Economic Consequences of Outdoor Air Pollution. OECD Publishing, Paris. https://doi.org/10.1787/9789264257474-en.

OECD (Organization for Economic Cooperation and Development), 2022. Metropolitan areas. Online: https://stats.oecd.org/Index.aspx?DataSetCode=CITIES. (Accessed 17 June 2022).

OpenStreetMap, 2023. OpenStreetMap Data Extracts Online. https://download.geofabrik.de/. (Accessed 3 March 2023).

Ortega, J.M., Rheinboldt, W.C., 1970. Iterative solution of nonlinear equations in several variables. Comput. Sci. Appl. Mathemat., University of Pittsburgh. https://doi.org/10.1016/C2013-0-11263-9.

Pérez-Invernón, F.J., Huntrieser, H., Erbertseder, T., Loyola, D., Valks, P., Liu, S., Allen, D.J., Pickering, K.E., Bucsela, E.J., Jöckel, P., van Geffen, J., Eskes, H., Soler, S., Gordillo-Vázquez, F.J., Lapierre, J., 2022. Quantification of lightning-produced NOx over the Pyrenees and the Ebro Valley by using different TROPOMI-NO$_2$ and cloud research products. Atmos. Meas. Tech. 15, 3329–3351. https://doi.org/10.5194/amt-15-3329-2022.

Rodgers, C.D., 2000. Inverse Methods for Atmospheric Sounding – Theory and Practice, Series on Atmospheric, Oceanic and Planetary Physics. World Scientific Publishing, Singapore, 2000.

Roesch, A., Schmidbauer, H., 2018. WaveletComp: Computational Wavelet Analysis. R Package Version 1.1. Online. https://cran.r-project.org/web/packages/WaveletComp.pdf. (Accessed 22 September 2020).

Roppongi, H., Suwa, A., Puppim De Oliveira, J.A., 2017. Innovating in sub-national climate policy: the mandatory emissions reduction scheme in Tokyo. Clim. Pol. 17 (4), 516–532. https://doi.org/10.1080/14693062.2015.1124749.

Russell, A.R., Valin, L.C., Cohen, R.C., 2012. Trends in OMI NO$_2$ observations over the United States: effects of emission control technology and the economic recession. Atmos. Chem. Phys. 12, 12197–12209. https://doi.org/10.5194/acp-12-12197-2012.

Seinfeld, J.H., Pandis, S.N., 2016. Atmospheric Chemistry and Physics. From Air Pollution to Climate Change, third ed. John Wiley & Sons, Inc., Hoboken, New Jersey, p. 1120.

Shah, V., Jacob, D.J., Li, K., Silvern, R.F., Zhai, S., Liu, M., Lin, J., Zhang, Q., 2020. Effect of changing NOx lifetime on the seasonality and long-term trends of satellite-observed tropospheric NO$_2$ columns over China. Atmos. Chem. Phys. 20, 1483–1495. https://doi.org/10.5194/acp-20-1483-2020.

Shen, H., Wang, Y., Deng, R., 2021. Can clean energy consumption promote the decoupling between economic growth and environmental pollution? – Spatial empirical analysis based on China. Pol. J. Environ. Stud 30 (4), 3787–3802. https://doi.org/10.15244/pjoes/131837.

Souri, A.H., Choi, Y., Jeon, W., Woo, J.-H., Zhang, Q., Kurokawa, J., 2017. Remote sensing evidence of decadal changes in major tropospheric ozone precursor over East Asia. J. Geophys. Res. Atmos. 122, 2474–2492. https://doi.org/10.1002/2016JD025663.

Spinu, V., Grolemund, G., Wickham, H., Lyttle, I., Constigan, I., Law, J., Mitarotonda, D., Larmarange, J., Boiser, J., Lee, C.H., 2018. Lubridate: make dealing with dates a little easier. Online: http://lubridate.tidyverse.org. (Accessed 2 March 2023).

Takashima, H., Irie, H., Kanaya, Y., Akimoto, H., 2011. Enhanced NO2 at Okinawa Island, Japan caused by rapid air-mass transport from China as observed by MAX-DOAS. Atmos. Environ. 45, 2593–2597. https://doi.org/10.1016/j.atmosenv.2010.10.055.

TMG (Tokyo Metropolitan Government), 2018. Tokyo Carbon reporting program for SMFs. Online: https://www.kankyo.metro.tokyo.lg.jp/en/climate/tokyo_carbon.html. (Accessed 3 March 2023).

TMG (Tokyo Metropolitan Government), 2018a. Tokyo Carbon reporting program for SMFs. TMG's Carbon Policy for SMEs (overview). Online. https://www.kankyo.metro.tokyo.lg.jp/en/climate/tokyo_carbon.files/TMGsCarbonPolicyforSMEs.pdf. (Accessed 3 March 2023).

TMG (Tokyo Metropolitan Government), 2018b. Tokyo Carbon reporting program for SMFs. Overview of Carbon reporting. Online: https://www.kankyo.metro.tokyo.lg.jp/en/climate/tokyo_carbon.files/OverviewofCarbonReporting.pdf. (Accessed 3 March 2023).

TMG (Tokyo Metropolitan Government), 2019. Zero Emission Tokyo Strategy. TMG Announces the „Zero Emission Tokyo Strategy" for Contributing to the World's Net-Zero CO2 Emissions by 2050. Online: https://www.kankyo.metro.tokyo.lg.jp/en/about_us/zero_emission_tokyo/strategy.html. (Accessed 3 March 2023).

TMG (Tokyo Metropolitan Government), 2019a. Zero Emission Tokyo Strategy. Revised Edition. Online: https://www.kankyo.metro.tokyo.lg.jp/en/about_us/zero_emission_tokyo/strategy.files/Full-ver.ZE-strategy0311.pdf. (Accessed 9 November 2022).

TMG (Tokyo Metropolitan Government), 2023. Tokyo cap-and-trade program. https://www.kankyo.metro.tokyo.lg.jp/en/climate/cap_and_trade/index.html. (Accessed 3 March 2023). Online.

Tokyo Statistical Yearbook, 2020. Population and Households. Table 2-1 Changes in Population. Online: https://www.toukei.metro.tokyo.lg.jp/tnenkan/2020/tn20q3e002.htm. (Accessed 2 November 2022).

Tong, D.Q., Lamsal, L., Pan, L., Ding, C., Kim, H., Lee, P., Chai, T., Pickering, K.E., Stajner, I., 2015. Long-term NOx trends over large cities in the United States during the great recession: comparison of satellite retrievals, ground observations, and emission inventories. Atmos. Environ. 107, 70–84. https://doi.org/10.1016/j.atmosenv.2015.01.035.

Torrence, C., Compo, G.P., 1998. A practical guide to wavelet analysis. Bull. Am. Meteorol. Soc. 79 (1), 61–78. https://doi.org/10.1175/1520-0477(1998)079%3C0061:APGTWA%3E2.0.CO;2.

United States Census Bureau, 2020. Population Census, April 1, 2020, San Bernardino County, Ventura County, Orange County, and Los Angeles County. Online: https://www.census.gov/quickfacts/fact/table/sanbernardinocountycalifornia,venturacountycalifornia,orangecountycalifornia,losangelescountycalifornia,CA/POP010220. (Accessed 5 July 2022).

USGS SRTM 1 Arc-Second Global, 2018. USGS EROS archive - digital elevation - shuttle radar topography mission (SRTM) 1 Arc-Second global. Earth Resources Observation and Science (EROS) Center. https://doi.org/10.5066/F7PR7TFT. (Accessed 3 March 2023).

Voigt, C., Lelieveld, J., Schlager, H., Schneider, J., Curtius, J., Meerkötter, R., Sauer, D., Bugliaro, L., Bohn, B., Crowley, J.N., Erbertseder, T., Groβ, S., Hahn, V., Li, Q., Mertens, M., Pöhlker, M.L., Pozzer, A., Schumann, U., Tomsche, L., Williams, J., Zahn, A., Andreae, M., Borrmann, S., Bräuer, T., Dörich, R., Dörnbrack, A., Edtbauer, A., Ernle, L., Fischer, H., Giez, A., Granzin, M., Grewe, V., Harder, H., Heinritzi, M., Holanda, B.A., Jöckel, P., Kaiser, K., Krüger, O.O., Lucke, J., Marsing, A., Martin, A., Matthes, S., Pöhlker, C., Pöschl, U., Reifenberg, S., Ringsdorf, A., Scheibe, M., Tadic, I., Zauner-Wieczorek, M., Henke, R., Rapp, M., 2022. Cleaner skies during the COVID-19 lockdown. Bull. Am. Meteorol. Soc. 103 (8), E1796–E1827. https://doi.org/10.1175/BAMS-D-21-0012.1.

Vrekoussis, M., Richter, A., Hilboll, A., Burrows, J.P., Gerasopoulos, E., Lelieveld, J., Barrie, L., Zerefos, C., Mihalopoulos, N., 2013. Economic crisis detected from space: air quality observations over Athens/Greece. Geophys. Res. Lett. 40, 458–463. https://doi.org/10.1002/grl.50118.

Wagner, N.L., Riedel, T.P., Roberts, J.M., Thornton, J.A., Angevine, W.M., Williams, E.J., Lerner, B.M., Vlasenko, A., Li, S.M., Dubé, W.P., Coffman, D.J., Bon, D.M., de Gouw, J.A., Kuster, W.C., Gilman, J.B., Brown, S.S., 2012. The sea breeze/land breeze circulation in Los Angeles and its influence on nitryl chloride production in this region. J. Geophys. Res. 117, D00V24. https://doi.org/10.1029/2012JD017810.

Wessel, P., Smith, W.H.F., 1996. A global, self-consistent, hierarchical, high-resolution shoreline database. J. Geophys. Res. 101 (B4), 8741–8743. https://doi.org/10.1029/96JB00104.

WHO (World Health Organization), 2022. Ambient (Outdoor) Air Pollution. https://www.who.int/news-room/fact-sheets/detail/ambient-(outdoor)-air-quality-and-health. (Accessed 9 September 2022).

Wickham, H., 2016. ggplot2: Elegant Graphics for Data Analysis. Springer-Verlag New York. Online: https://ggplot2.tidyverse.org/. (Accessed 2 March 2023).

Wood, S.N., 2017. Generalized Additive Models. An Introduction with R, second ed. Chapman and Hall/CRC, New York. https://doi.org/10.1201/9781315370279.

World Settlement Footprint (Wsf), 2019. Online: https://geoservice.dlr.de/web/maps/eoc:guf:3857. (Accessed 3 March 2023).

Wu, Y., Zhou, Y., Xu, B., 2022. Decoupling relationship between economic growth and PM2.5 emissions in the transportation sector in China: regional differences and influencing factors. Environ. Res. Lett. 17 (4), 044065 https://doi.org/10.1088/1748-9326/ac5f2b.

Wuest, S., Bittner, M., 2006. Non-linear resonant wave-wave interaction (triad): case studies based on rocket data and first application to satellite data. J. Atmos. Sol. Terr. Phys. 68 (9), 959–976. https://doi.org/10.1016/j.jastp.2005.11.011.

Yu, B., Fang, D., 2021. Decoupling economic growth from energy-related PM2.5 emission in China: a GDIM-based indicator decomposition. Ecol. Indicat. 127, 107795 https://doi.org/10.1016/j.ecolind.2021.107795.

Zhang, R., Zhang, Y., Lin, H., Feng, X., Fu, T.-M., Wang, Y., 2020. NOx emission reduction and recovery during COVID-19 in East China. Atmosphere 11 (4), 433. https://doi.org/10.3390/atmos11040433.

Zhou, W., Yang, D., Xie, S.-P., Ma, J., 2020. Amplified Madden-Julian oscillation impacts in the Pacific-North America region. Nat. Clim. Change 10, 654–660. https://doi.org/10.1038/s41558-020-0814-0.